Master's thesis

NTNU
Norwegian University of Science and Technology
Faculty of Medicine and Health Sciences
Department of Clinical and Molecular Medicine

Hoang Ha My Dang

Exploring responses of type I and type III interferons in human macrophages

Master's thesis in Molecular Medicine
Supervisor: Marit Walbye Anthonsen
June 2021

NTNU
Norwegian University of
Science and Technology

Hoang Ha My Dang

Exploring responses of type I and type III interferons in human macrophages

Master's thesis in Molecular Medicine
Supervisor: Marit Walbye Anthonsen
June 2021

Norwegian University of Science and Technology
Faculty of Medicine and Health Sciences
Department of Clinical and Molecular Medicine

NTNU
Norwegian University of
Science and Technology

Abstract

Interferons are antiviral cytokines induced during viral infection. Type I and III IFNs are thought to share some of the same transcriptional outputs, yet some biological responses are distinct. IFN-λ receptor (IFNLR1) expression is not ubiquitous like the type I receptor and is strongly expressed in epithelial cells such as the respiratory tract and intestine. The molecular mechanisms underlying the different biological effects and cell-specific responses of type I and type III IFN are poorly understood. The extent to which type III IFNs can affect immune cells is controversial. This work aimed to investigate if human primary monocyte-derived macrophages (MDMs) express IFNLR1, whether IFN-λ1 induces antiviral and innate immune genes, and has antiviral activity against respiratory virus human metapneumovirus (HMPV) and its IFN-λ1 effects depend on IFNLR1 in MDMs. We found that type III IFNs were induced in response to HMPV infection in MDMs. Also, we found that human MDMs exhibit higher expression of both sIFNLR1 and mIFNLR1 compared with the analyzed epithelial cell types. At 24 hours post-exposure, pretreatment with type III reaches maximal ISG induction earlier than IFNs type I. 48-hour pretreatment with type I IFNs and III is able to reduce HMPV replication after 48-hour infection. Our result showed that type I and III IFNs induce a similar subset of ISG genes, but with differences in potency and kinetics. Type III IFN is slower and weaker in ISG induction, and could be less inflammatory and may provide therapeutic benefits with fewer side effects compared to type I IFN. siRNA-mediated reduction of IFNLR1 level significant suppress Viperin expression with concomitant increase in CXCL-10 and inflammatory cytokine IL-6. Also, we found that the JAK/STAT inhibitor Ruxolitinib can inhibits IFN-λ1-induced ISG pathways in human MDMs. Collectively, these results suggest that human MDMs express a functional IFNLR1.

Acknowledgments

I would like to express my gratitude to my Professor Marit Walbye Anthonsen for providing guidance and feedback throughout this project. I would particularly like to thank to Ph.D. student Alix Saskia Spahn for being patiently teaching me all necessary lab techniques, answering all my questions, and providing helpful advice. I would also like to thank to the Lab technician Kristin Rian for technical supports on my study. Without their assistant, this thesis would have never been accomplished.

Finally, I would like to express my gratitude to my new friends in Norway and especially to my family both in Vietnam and Denmark. Without their understanding and encouragement in the past few years, it would be impossible for me to complete my study.

Trondheim, May 30th, 2021
Hoang Ha My Dang

Abbreviation

HMPV	human metapneumovirus
IFN-λ	interferon lambda
IFN-β	interferon beta
RTI	respiratory tract infections
URTI	upper respiratory tract infections
LRTIs	lower respiratory tract infections
ARI	acute respiratory illnesses
RSV	respiratory syncytial virus
HMPV	human metapneumovirus
RV	rhinovirus
HPIV	parainfluenza virus
Flu	influenza virus
CoV	coronavirus
APV	Avian pneumovirus
ssRNA	sense single-strand RNA
NF-kB	nuclear factor-kB
RDRP	RNA-dependent RNA polymerase
ER	endoplasmic reticulum
IFN	Interferon
PRRs	pattern recognition receptors
ISGs	interferon-stimulated genes
IFNR	IFNs receptor
mIFNLR1	membrane-associated receptor
sIFNLR1	soluble-associated receptor
PAMP	pathogen-associated molecular patterns
TLRs	Toll-like receptors
CLRs	C-type lectin receptors
NLRs	NOD-like receptors

RLRs	RIG-I-like receptors
DAMPs	damage-associated molecular patterns
MDA5	melanoma differentiation-associated 5
IRF	IFN regulatory factor
TRIF	TIR-domain-containing adapter-inducing interferon-β
MyD88	Myeloid differentiation factor 88
JAK	Janus kinase
TYK	Tyrosine Kinase
STAT	signal transducer and activator of transcription
ISGF	interferon-stimulated gene factor
ISRE	IFNs-stimulated response element
MHC	major histocompatibility complex
Viperin	Virus inhibitory protein, endoplasmic reticulum-associated, interferon-inducible
RSAD2	Radical S-Adenosyl Methionine Domain Containing 2
Cig5	Cytomegalovirus inducible gene 5
CDSs	cytosolic DNA sensors
MAVS	Mitochondrial antiviral-signaling protein
FPPS	farnesyl diphosphate synthase
HCV	hepatitis C virus
WNV	West Nile virus
DENV	dengue virus
HCMV	human cytomegalovirus
HIV	human immunodeficiency virus
CHIKV	Chikungunya virus
CH25H	Cholesterol-25-hydroxylase
25HC	25-hydroxycholesterol
SREBPs	sterol-responsive element-binding protein
MDMs	monocyte-derived macrophages
LLC-MK2	Lilly Laboratories Cell-Monkey Kidney 2
PBMCs	peripheral blood mononuclear cell

siRNAs	short interfering RNA
RUX	Ruxolitinib

Table of Contents

1 Introduction

1.1 Overview

A significant cause of morbidity and mortality worldwide is acute respiratory tract infections (RTIs), which are considered to be upper respiratory tract infections (URTIs) and lower respiratory tract infections (LRTIs) [1]. Occurrence rates showed an analogous pattern in children under five years old in both developed and developing countries, but with a higher mortality rate in the latter [2]. The study by Williams and his group revealed that within the year 2000 about 1.9 million infants and toddlers died worldwide as a consequence of acute respiratory illnesses (ARI), 70% of whom came from Asia and Africa. [1, 3]. Viral pathogens, like the human respiratory syncytial virus (RSV), human metapneumovirus (HMPV), rhinovirus (RV), parainfluenza virus (HPIV), influenza virus (Flu), and coronavirus (CoV) are the foremost prevalent reason behind RTIs [2].

1.2 Human Metapneumovirus (HMPV)

In 2001, Bernadette and his group isolated a newly Pneumovirus, HMPV, from nasal samples of 28 children suffering from RTIs. It is accountable for a large proportion of infant mortality worldwide and becomes the second most identified pathogen after RSV. Indeed, infants have the highest rate of received hospital care due to HMPV infection. Antibody testing for HMPV indicated that the virus had been exposed to children at an early age of five and had been existed for many decades, even before its identification unveil [4, 5].

HMPV is distributed globally and is found in all continents [6]. In temperate and tropical regions, HMPV occurs simultaneously with the other respiratory virus annually in winter and early spring. It is observed that its peak of the activity regarding location is somewhat later than with RSV and influenza [5, 7-9]. In some places, HMPV can be detected all year round even though it expresses lower levels after spring until the fall season, especially in August and September (Figure 1). Owing to the fact that the transmission depends on several factors such as the surrounding

environment and host, there are a few concrete studies on HMPV transmission routes [10]. It is, nonetheless, assumed that its transmission is analogous to other RTIs and is transmitted directly or indirectly via airborne, e.g., by droplets, saliva, or aerosols [11]. Besides, on non-absorbing materials, HMPV is stable and can scarcely recover even on absorbent subjects [10, 12]. Despite the very fact that HMPV is principally recognized as a source of RTIs in children, it is likewise a significant cause of RTIs in adults, especially in immunocompromised patients and the elderly both healthy and illness states. Symptoms can develop from mild URTIs to a debilitating effect on bronchiolitis and pneumonia [2, 7, 11].

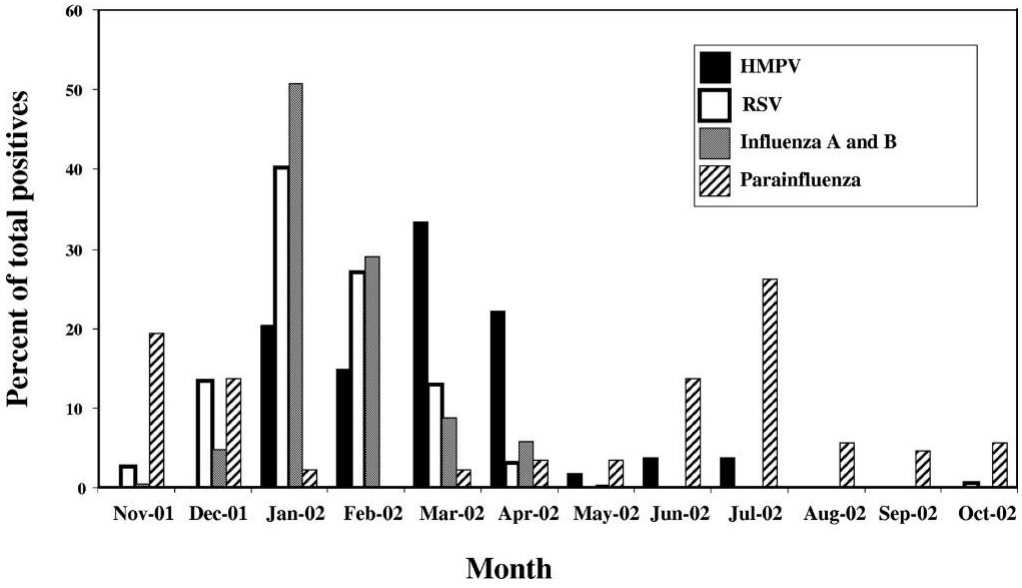

Figure 1 Seasonal distribution of HMPV and other respiratory viruses RSV, Influenza A and B, and Parainfluenza. The total positive cases are shown as the percentage. Source: © 2004 by the Infectious Diseases Society of America [6]

1.2.1 Molecular Virology

HMPV is labeled as species *Human metapneumovirus*, which belongs to genus *Metapneumovirus*, within the *Pneumoviridae* family, includes RSV. Avian pneumovirus (APV) is the nearest genetic relative [5, 9, 11].

In the Baltimore classification system, HMPV is positioned in group V, owing to its negative-sense single-strand RNA (ssRNA). The virion consists of a defined lipid envelope where three different viral glycoproteins are embedded, and enclosed a helical nucleocapsid (Figure 2a). Its non-segmented ssRNA genome has a length around 13kb in size and consists of eight genes that

encode for nine proteins. These comprise nucleocapsid protein (N), phosphoprotein (P), matrix protein (M), fusion protein (F), matrix protein (M2-1, M2-2), small hydrophobic protein (SH), glycoprotein (G), and polymerase (L) (Figure 2b) [5, 9, 11]. In which three glycoproteins, F protein liable for the fusion between the host membrane and the viral, G in charge as the attachment protein whilst the role of the SH protein remains uncleared [9]. Some research proposed that SH regulates membrane permeability [13, 14] while others indicated that SH supports the regulation of host innate and acquired immunity by ceasing the activation of nuclear factor-kB (NF-kB), a pivotal mediator of pro-inflammatory genes [14-16]. The viral N protein similarly encapsulates the ssRNA as the RSV with the adornment of the P, L, and M2-2 proteins, which participate in the viral replication and transcription [9, 14]. Two distinct lineages of HMPV had been classified as A and B via the phylogenetic analysis. This classification depends on the sequence variability between genes encoding for F, G, L, M, and N proteins [9, 11]. Each type is further designated into sub-groups termed A1, A2, B1, and B2 based on the sequence diversity of surface glycoproteins G and F [9, 11].

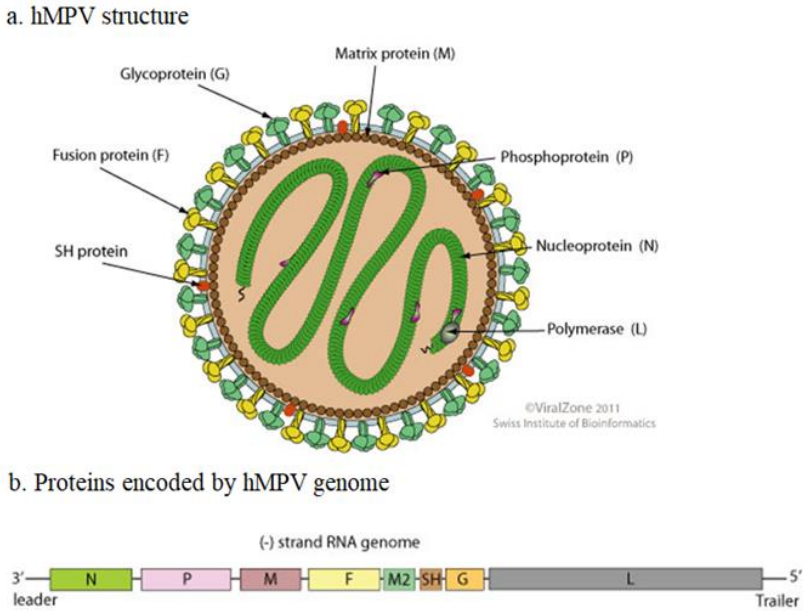

Figure 2 HMPV molecular structure with protein-coding from its genome. The figure show (a) viral structure model with lipid enveloped, the spherical shape makes from materials encoded by (b) HMPV linear genome. Source: [17]

1.2.2 Viral Replication

Ciliated epithelial cells in the airways, such as those in the nose and lungs, are the primary target of the virus for its attachment. Since HMPV homologous with the rest of the *Paramyxoviridae* family, its viral life cycle entails the elementary steps that resemble the other negative ssRNA viruses in particular RSV.

To infect the cell, the virus uses the G protein to attach to the host's cellular receptor and then the F protein to mediate the entry of the nucleocapsid into the cytoplasm by fusing their membrane with host cell membranes [18, 19]. After this event, the viral genome is discharged into the cytoplasm, where proteins P, N, and L detach from the viral RNA and assemble into the polymerase complex. This complex together with M2 (M2-1, M2-2) begins transcription, and the viral genome can be translated into viral proteins by the ribosomes of the host cell. In this process, M2-1 protein regulates the viral transcription by preventing pre-mature termination whereas M2-2 protein is a regulatory factor that switches the RNA-dependent RNA polymerase (RdRp) from mRNA to vRNA [17, 20, 21]. Alternatively, the genome is replicated to produce the antigenome after initial transcription, which produces a full-length positive-strand template for replication and further production of the negative-strand RNA genome. After translation, all essential proteins F, G, and SH are transported from the endoplasmic reticulum (ER) to the Golgi apparatus, and then to the plasma membrane to become the new surface glycoproteins. In the meanwhile, the M protein is transported directly forward to the plasma membrane and wait there until the other components are ready to assemble. Eventually, newly formed viral progeny can release themself from the plasma membrane via the budding mechanism (Figure 3) [5, 17, 19].

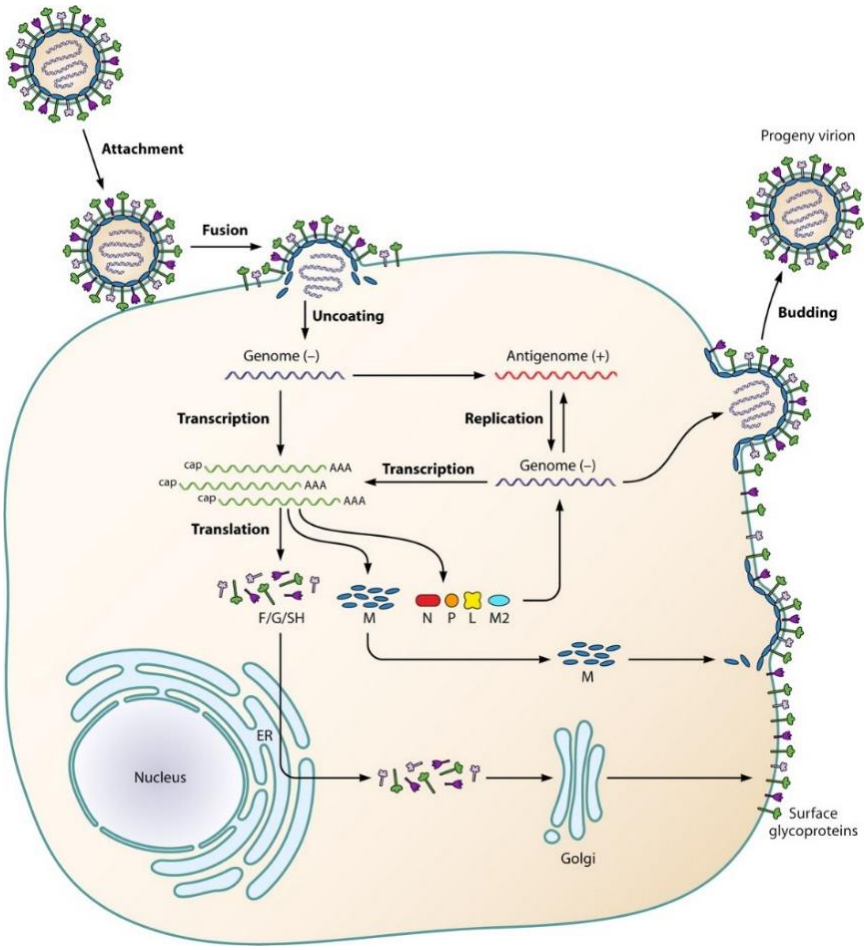

Figure 3 HMPV life cycle. The virus attaches to cell surface receptors, un-coats, and releases the negative-sense viral RNA into the cytoplasm, where it intermediate commences the transcription and translation. Following this is the production of positive-sense RNA for protein synthesis and genome reproduction afterward. Specific viral proteins, such as F/G/SH are produced and transmitted to ER and Golgi, correspondingly, while M protein is transported to the plasma membrane. Once new virions are formed, it is prone to dispatch by budding from the host cell. Source: [17]

1.3 The Interferon (IFN) System

Interferons were first discovered in the mid-1930s but during that time, its conception quite different from today's knowledge. Then in 1957, Isaacs and Lindenmann conducted research by infected choroid fragments from chicken embryos with inactivated influenza viruses. They obtained the supernatant from these infected cells and observed its protein production, which displayed the ability to protect the nearby cells against reinfection by the live virus. From that time, the name ‘interferon’ was originated from the ability to interfere with viral replication [22]. As of today, the interferon knowledge had been gathered and perfected through many studies with fine details and efforts. Subsequently, interferons are considered as a member of regulatory

protein also known as a cytokine and expressed by a diverse group of genes in response to viral infection [23, 24].

In general, when HMPV invades the human body, the first physical barrier and target are the epithelial linings of the respiratory tract and the lungs. Once the intruder breaks through the anatomical barriers, cellular responses are activated, and the virus is detected by pattern recognition receptors (PRRs). This recognition is followed by the release of IFNs, which is induced by cells of the immune system such as macrophages, and dendritic cells etc.… in reaction to the infection that comes from virus, bacteria, or parasites. The IFNs act antivirally in several ways when its respective receptor is activated, leading to downstream reactions. The IFN-mediated reaction prevents virus replication through its production from the interferon-stimulated gene (ISGs) [25].

1.3.1 Interferon Classification

Despite the early discovery of IFNs in 1957, the family of interferons was not completely revealed at once, some of them are just recently discovered. In the mammal, three types of IFNs have been classified based on their amino acid sequence homology and their receptors. Each IFNs family member modulates the host response to viral activity through its corresponding IFNs receptors [26].

Type I IFNs, a viral IFN that represents a large family of cytokines comprising various subtypes α (leukocytes), β (fibroblast), τ (trophoblast), ω (leukocytes), ε, δ, κ, and ζ [23, 26]. Those genes are located on chromosome 9, single-exon genes, and nearly all cell types can provoke a type-I IFN response. Still, during the infection stage, one specialized type of immune cell referred to as plasmacytoid dendritic cells induce a high amount of IFN-α [27]. It signals through the heterodimeric IFN-α/β receptor (IFNAR), comprised of IFNAR1 and IFNAR2 subunits, where it binds IFNAR2 first with high affinity then lately recruits the low-affinity IFNAR1 [26, 28-30].

Type II IFNs an immune IFNs that quite different from the other IFNs because it has only one subtype γ, and not stimulate by sensing of virus fragments but by mediated predominantly by natural killer T (NKT) and natural killer (NK) cells [26]. Its genes are located on chromosome

12, contain three introns [22, 24]. Cellular response to IFN-γ signaling through heterodimeric IFN-γ receptor (IFNGR1 and IFNGR2), which are widely expressed, and thus almost all cell types can respond to IFN-γ [22, 26, 27], but in this research, it will not be the main attention.

Type III IFNs have currently been discovered in 2003 [31], including four isoforms: λ1 (interleukin (IL)-29), λ2 (IL-28A), λ3 (IL-28B), and recently identified λ4. Those genes are located on chromosome 19, including five exons and four introns. IFNs type III binds IFNLR1 first with high affinity then lately recruits the low-affinity IL10Rβ [23, 27, 29, 30, 32].

The IFNLR1 receptor chain contains at least two splice variants that had been reported in Shepard's research: a membrane-associated variant (mIFNLR1), which lacks a part of exon VII causing a 29 amino-acid deletion within the intracellular domain and a truncated soluble receptor (sIFNLR1), which misses entire exon VI within transmembrane domain result in a premature stop codon as the consequence of a frameshift (Figure 4) [33-35].

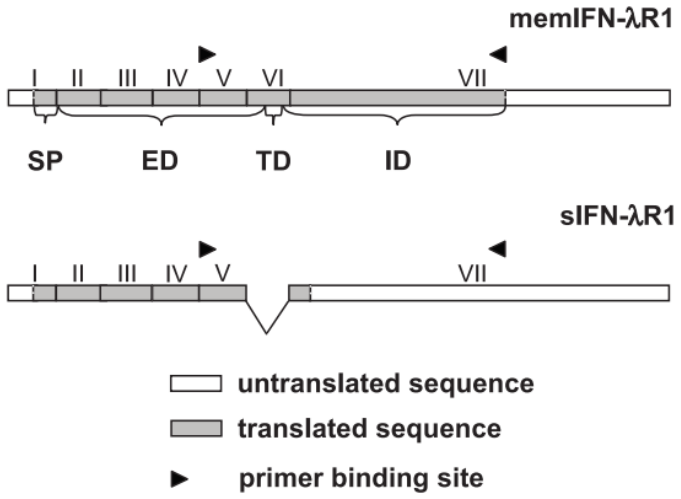

Figure 4 Illustration displays the difference between two splice variants of the IFNLR1 receptor chain: membrane-associated receptor chain (mIFNLR1) as the full-length form and truncates soluble receptor (sIFNLR1) as the shorter form is due to the missing of exon VI. For mIFNLR1, the predicted protein domains are shown from left to right, as follows: signal peptide (SP), extracellular domain (ED), transmembrane domain (TD), and intracellular domain (ID). Source: [33]

1.3.2 Induction of Interferon Response by Pathogenic Viruses

Upon viral infection, cells use receptors called PRRs detect pathogen-associated molecular patterns (PAMP), that are associated with pathogen infection [36]. These receptors PRRs are divided into groups based on their localization: membrane-bound PRRs (Toll-like receptors

(TLRs) and C-type lectin receptors (CLRs)), cytoplasmic PRRs (NOD-like receptors (NLRs) and RIG-I-like receptors (RLRs)), and secreted receptors [37]. Besides PAMP, when the virus-induced cell lysis it releases damage-associated molecular patterns (DAMPs) which originated from host cells. These two major pathways play an essential role in the innate immune response against HMPV.

The first pathway involves PRRs in cytoplasm like RLRs which include RIG-I (retinoic acid-inducible gene I and melanoma differentiation-associated 5 (MDA5) responsible for sensing viral genomes ssRNA, or dsRNA generated through the virus replicative cycle. Upon the recognition, RLRs activate MAVS which subsequently activates downstream IFN regulatory factor 3 (IRF3), following the secretion of type I IFN, upregulation of IRF7, and NF-kB. This sequentially triggers the secretion of proinflammatory cytokines and type III IFNs [14, 36].

Endosomal TLRs such as TLR3 (dsRNA), TLR7, TLR8 (ssRNA) involve in the second pathway for sensing HMPV, which leads to the activation of IRF3 via the adaptor protein TIR-domain-containing adapter-inducing interferon-β (TRIF), and IRF7 via the adaptor protein Myeloid differentiation factor 88 (MyD88) [14, 36]. This further triggering the expression of IFNs.

The recognition of viral PAMPs through PRRs triggers the activation of a variety of signaling cascades that promote IFN expression (Figure 5) [30, 36]. The form of IFN produced can be affected by the subcellular location where the PAMP involvement. For instance, for TLR4, it has been suggested that the production will be IFNs type I if it involves endosomes, while its product will be IFNs type III if it involves the plasma membrane [30].

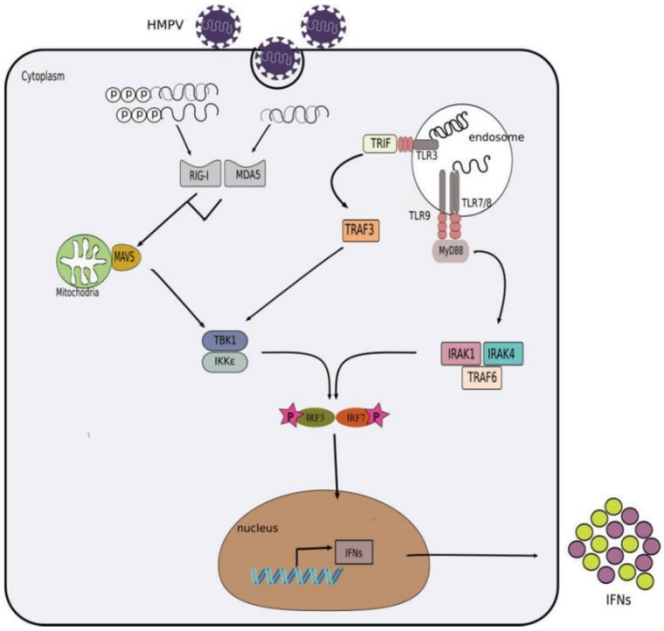

Figure 5 Interferon induction by HMPV. When the virus infects the cell, its PAMPs are recognized by toll-like receptors (TLRs) and RIG-I-like receptors (RLRs) in the endosome and cytoplasm, respectively. Upon viral ssRNA recognition, TLR7/8 activates and in turn recruits the adaptor molecule myeloid differentiation primary response protein 88 (MyD88). The activation of MyD88 leads to the recruitment of interleukin 1 receptor-associated kinases (IRAK1 and IRAK4) and the tumor necrosis factor receptor-associated factor 6 (TRAF6). This combination sequentially mediates the phosphorylation and activation of IRF7 which translocate to the nucleus to initiate the expression of IFNs. In the case of dsRNA as a product of viral replication, it can be sensed by TLR3 in the endosome, and it facilitates the complex formation of TANK-binding kinase 1 (TBK-1) and I kappa B kinase epsilon (IKK-ε) that ultimately leading to activation of IRF3/7. Also the complex TBK-1/ IKK-ε can be activated by dsRNA viruses by RIG-I and MDA5 which bind and activate MAVS. This activation furthers the signaling cascade and ¨promote cytokine production. Source: [36, 38]

1.3.3 Interferon Signaling

The downstream signaling and transcriptional responses activated by IFNs type I and III have significant similarities regardless of their different receptors [30]. An immune response mediated by IFNs can be activated by both IFNs type I and III when it binds to their IFNRs on the cell surface via autocrine or paracrine signaling [39]. The binding of either IFNs type I or type III results in the activation of Janus kinase 1 (JAK1) and Tyrosine Kinase 2 (TYK2) kinases, followed by phosphorylation of heterodimers signal transducer and activator of transcription STAT1 and STAT2 [30, 34, 40, 41].

Phosphorylated STATs associate with interferon regulatory factor 9 (IRF9) to create an interferon-stimulated gene factor 3 (ISGF3) transcription complex. This complex transposes to the nucleus and binds to an identified IFNs-stimulated response element (ISRE) in the upstream promoter of specific IFN-responsive genes which in turn, encode proteins that work via a range

of mechanisms to constrain viral infection [34, 40, 41]. As a result, ISGF3 activation leads to the induction of similar signaling pathways and transcriptional responses regardless IFNs type I or III (Figure 6). However, unique signaling pathways and distinct magnitude and kinetics of signaling are also enabled for type I and type III IFNs. Such signaling of IFNs type I is stronger, transient, more rapid induction but quickly declines ISGs which contrasts with the IFNs reaction of type III [30, 39, 41].

Furthermore, IFNs additionally play a role in the upregulation of the major histocompatibility complex and increasing immunoproteasome activity. More specifically, higher major histocompatibility complex MHC I and MHC II increase binding and present virus-derived peptide fragments on the cell surface so that CD8+ and CD4+ T cells can recognize them [42]. The immunoproteasome responsible for processing the viral peptides before they are loaded onto the MHC I molecule then promotes the recognition and destruction of infected cells. [43].

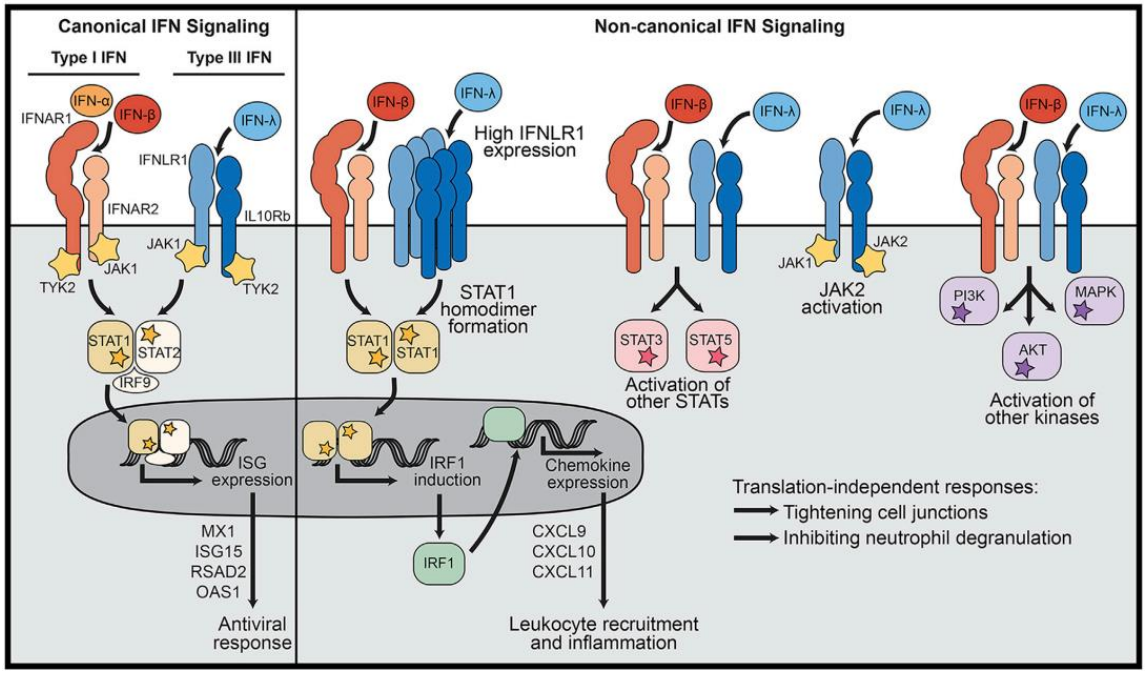

Figure 6 Model of signaling pathways for IFN type I and III. On the left, the schematic represents the canonical pathway. Upon the biding to IFNLR or IFNAR, the dimerized receptors activate TYK2 and JAK which further initiate the phosphorylation of STAT1 and STAT2. Those phosphorylated STAT proteins will recruit the IRF9 to form the ISGF3 complex. Afterward, this complex translocates into the nucleus and acts as a transcription factoring to promote the expression of ISGs. Besides the canonical pathway, both IFNs types I and III can also signal through other STATs (STAT1 homodimers, STAT3, STAT5) and kinases (PI3K, AKT, and MAPK). Those are denoted as non-canonical signaling pathways. Source: [41]

1.3.4 Interferon-Stimulated Genes (ISGs)

It is quite complex to answer the question of what all these ISGs are and what they all do. The easiest explanation for ISGs is that they are the genes that are produced during an IFNs response [44]. IFNs are important antiviral cytokines that maintain antiviral cellular status by upregulating the expression of ISGs [45].

Each phase of the virus infection, pathway, and functions needed during the viral life cycle possibly becomes the target for ISGs [27]. Its potent antiviral effect can further enhance the immune system via amplifying the production of IFNs or ISGs. Besides its ability to act as direct antiviral effectors as abovementioned, there are some well-known ISG activities including:

- Strengthen IFN signaling and prime cells for increased pathogen detection (PRRs and IRFs) and innate immune signaling [27].
- Mediated the IFN-desensitized state which allows cells to recover from IFN signaling after exposure, avoid the prolonged stimulus. One of its mechanisms negatively regulates IFN signaling by inhibiting the JAK/STAT signaling pathway [27].

Here is the emphasis on the function of two highlighted ISGs.

Virus inhibitory protein, endoplasmic reticulum-associated, interferon-inducible (Viperin):

Viperin, also known as Radical S-Adenosyl Methionine Domain Containing 2 (RSAD2) or Cytomegalovirus inducible gene 5 (Cig5), has recently attracted a lot of attention [46, 47]. It is induced by many cell types as a product of ISGs, which are triggered by type I, II, and III IFNs and possess antiviral activity in combat against dsRNA and DNA viruses [46, 48]. The gene itself can be triggered by one of two innate immune pathways: JAK/STAT signaling or IRF3 activation.

For IFNs dependent signaling, the activation of PRRs such as Toll-like receptor (TLR3/4), cytosolic DNA sensors (CDSs), and RIG-I-like receptors (RLR) lead to the secretion of IFNs. As the result, IFNs biding to the IFNR on the cell surface via autocrine or paracrine signaling activate the JAK/STAT pathway [48]. Subsequently, the signaling leads to the formation of the STAT1/STAT2/IRF9 complex also known as IFN-stimulated gene factor 3 (ISGF3) that bounds

to Interferon Stimulation Response Element (ISRE) and induce the transcription of Viperin (Figure 7)[42, 46, 48].

IFNs-independent pathway triggers ISGs expression directly via IRF3. Mitochondrial antiviral-signaling protein (MAVS) can be found in the outer membrane of both peroxisomes and mitochondria. Peroxisomal MAVS acts prematurely to prevent viral replication before the mitochondrial MAVS gets involved, which has a more intense and prolonged antiviral effect [47]. Additionally, MAVS is the adapter molecule downstream of the retinoic acid-inducible gene I (RIG-I) involves in the phosphorylation of interferon response factors 3 (IRF3) [27, 48]. IRF3 that has been phosphorylated transfer to the nucleus, where it attaches to the ISREs that are directly activating Viperin expression (Figure 7).

Viperin is a fascinating protein with antiviral activity against a wide variety of viruses. For instance, influenza virus, hepatitis C virus (HCV), West Nile virus (WNV), dengue virus (DENV), human cytomegalovirus (HCMV), HIV-1, and Chikungunya virus (CHIKV) [48, 49]. The one thing these viruses have in common is that they all have RNA genomes [49]. The ability to inhibit virus replication has been discovered on the Influenza virus by Wang et al. and his groups, who observed an atypically large amount of distinct stalk-like structure when new viral budding from lipid rafts—lipid microdomains with specific membrane [27, 46, 50]. Lipid rafts are critical sites where viral budding occurs, which means a disruption at this stage can prevent the release of viral particles [47]. Viperin accomplishes this by binding to and inhibiting farnesyl diphosphate synthase (FPPS), a key enzyme in isoprenoid biosynthesis, and impede FPPS activity modifies membrane fluidity, in that way intervene with virus budding [27, 47, 48, 51]. However, HCV, a virus that does not bud from lipid rafts, still be inhibited by Viperin [47]. Therefore, the mechanism of how exactly this protein affects replication in these cases stays uncleared but still, its high expression in different cell types under a wide spectrum of the virus suggests that this gene plays a crucial role in antiviral defenses [47, 48].

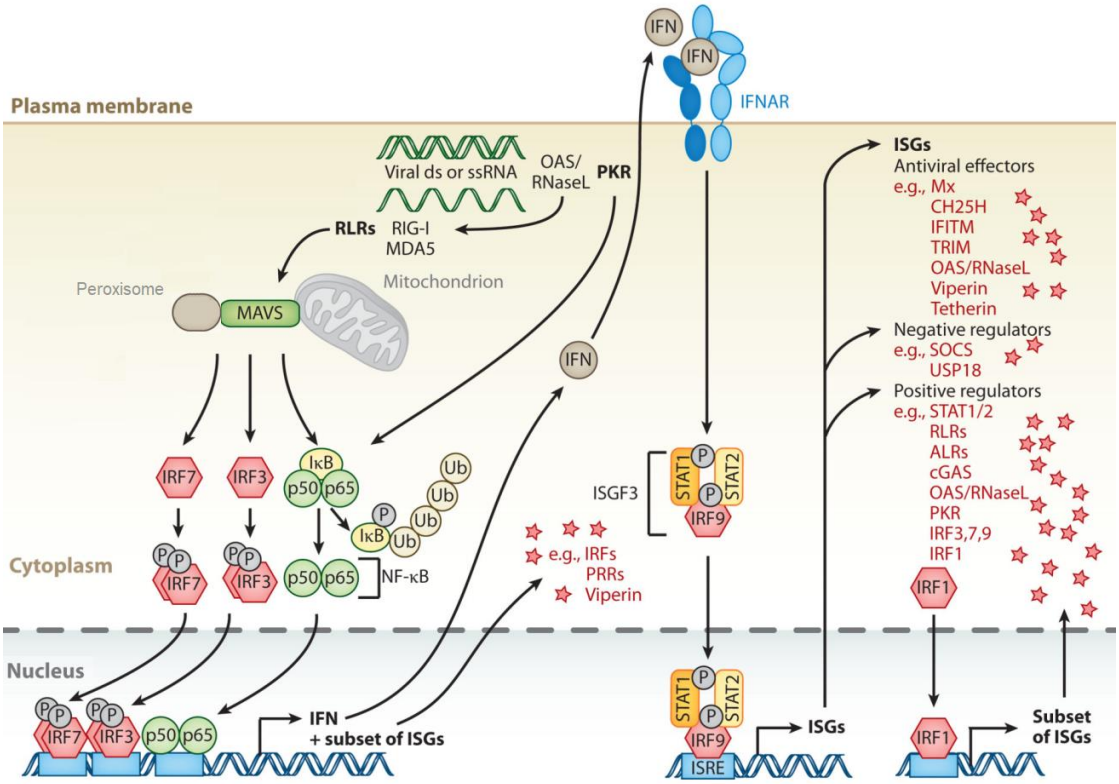

Figure 7 Viperin upstream signal regulation. Viperin induction is activated by the IFNs dependent pathway (right) and the IFN-independent pathway (left). The IFNs dependent pathway (JAK/STAT) is regulated by ISGF3, a complex combined with phosphorylated STAT and IRF9. The complex is then translocated to the nucleus and binds to the ISRE promoter and triggers the ISGs expression. These ISGs can be classified into antiviral effectors that include Viperin, negative regulators, and positive regulators. While IFN-independent is regulated by IRF3 and IRF7. Upon viral infection, viral genome ds or ssRNA is recognized by the RNA specialized PRRs such as RIG-I-like receptors (RLR)—RIG-I and MDA5. Then signaling via the mitochondrial adaptor protein MAVS at the peroxisome and mitochondrion outer membrane activates and phosphorylates the interferon response factors 3 or 7 (IRF3/7) and nuclear factor kappa-light-chain-enhancer of activated B cells (NF-κB). This leads to the nuclear translocation of IRF3/7 and NF-κB which are bound to the promoter and facilitates the expression of ISGs, includes Viperin. Source: [27].

Cholesterol-25-hydroxylase (CH25H):

An ER-associated glycoprotein encoded by an intronless gene, which is conserved across mammalian species. Both type I and type II IFNs can trigger CH25H expression [27, 45, 52]. Most CH25H locates in the endoplasmic reticulum (ER) and Golgi complex and converts cholesterol into oxysterol 25-hydroxycholesterol (25HC), a hydroxylase enzymatic product [27, 53]. CH25H plays a role as an antiviral IFN-dependent gene with the antiviral ability via its production, 25HC. This ability is not exclusively restricted to viral fusion blocking [27, 45, 54].

Furthermore, its antiviral effect is quite across the board, which was proved through the 25CH's effect test on various viruses even though its mechanism has not been fully unveiled. Yet, the result was quite impressive that CH25H-induced 25HC can inhibit the viral activity against a variety of enveloped DNA and RNA viruses, but unfortunately showed an exception in the non-enveloped virus [45]. Some studies showed that macrophages, as well as dendritic cells, are potentially a rich source of inducible CH25H as an innate immune system when exposing to the TLR3/4 agonists and IFNs [45, 54, 55]. Even though these investigations agreed on the role of 25-HC as an antiviral mediator, still they disagreed on the mechanism [52].

There is some suggestion for 25HC's mechanism in antiviral activities. One of them proposed that a high 25HC level increases cholesterol ester formation in cells, which modifies the target cell membrane's physical properties resulting in preventing virus-host membrane fusion [27, 45, 52]. The mechanism behind this is that 25HC can permeate through the membranes and directly modify them. Lange et al. and Olsen et al. both similarly confirmed the effect of 25H in increasing cellular cholesterol accessibility by directly mobilizing cholesterol from membranes and subsequently stop cholesterol from stiffening [45, 56, 57]. Liu et al. likewise agreed with the hypothesis that interactions of the hydroxyl groups of 25HC can result in membrane expansion and aggregation (Figure 8) [27, 45].

Another proposal is related to the regulation of the sterol biosynthesis pathway which partially controls by CH25H's product [27]. In general, sterol-responsive element-binding protein (SREBPs) can be regulated by natural oxysterol 25HC [42, 45, 54, 55]. The levels of SREBP are closely regulated via the negative feedback process by sterol biosynthesis products. This means an exceeding in sterol leads to 25HC accumulation will inhibit the sterol biosynthesis process and subsequently deplete cholesterol and isoprenoid, with the latter is crucial for protein prenylation (Figure 8) [27, 58]. These two sterols are required for the virus to synthesize essential components during the replication process and bud out by utilizing raft lipids [27, 58].

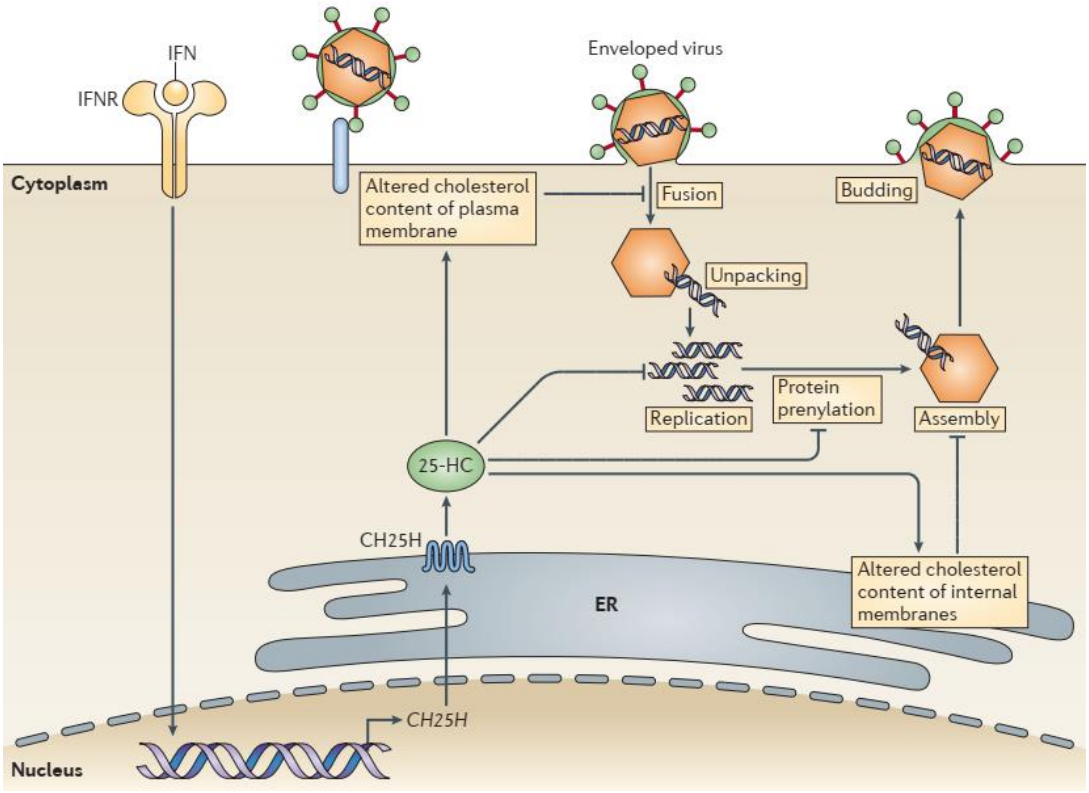

Figure 8 Illustration exhibit how CH25H involve in antiviral host defense. Signaling downstream from the interferon receptor (IFNR) triggers CH25H expression that promotes increased cholesterol production by 25-HC. Several studies have proposed antiviral effects of 25-CH as follows: altered cholesterol content of plasma membrane to inhibit viral fusion; disaffect viral and prenylation protein to block viral replication and assemble; altered cholesterol content of internal membranes to disrupt the membrane structure that is essential in viral assembly and genome packaging. Source: [52]

1.3.5 Modulation of the Interferon Response by HMPV

The interferon response is so vital for restraining the expression of HMPV so that it evolves in a way to stop the secretion of IFN type I. This secretion of type I IFNs pathway had been mentioned above included the RLR family and endosomal TLR3 and TLR7. To halt the type I IFN secretion, the SH protein of HMPV can inhibit STAT1 phosphorylation and eventually inhibiting numerous ISGs transcription [59, 60]. In addition, M2-2, P, G protein can impair the ability of RIG-I to recognize 5′-triphosphate viral RNA thereby weakening the expression of IFN-I and ISGs via an unknown mechanism [14]. Thus, suggests that HMPV can found some ways to interfere with signal transduction downstream of IFNRs.

1.4 Aims of The Study:

The molecular mechanisms underlying the different biological effects and cell-specific responses of type I and type III IFNs are poorly understood. Nevertheless, such information is important for the use of different IFNs in antiviral approaches, therapeutic strategies, and vaccine development.

This MSc project aimed to characterize and compare innate immune and antiviral signaling stimulated by type I and type III IFNs, and to address the involvement of proteins that are known to modulate metabolism in human MDMs, which were chosen as a model system. More specifically, the following sub-aims were pursued:

- Determine the expression of the IFNLR1 and evaluate MDMs responsiveness to the IFN type I and III signaling
- Establish the antiviral effect of type III IFNs compared to type I IFNs on MDMs infected by HMPV
- Explore the effect of type I and type III IFNs on CH25H, a protein related to immunometabolism.

2 Materials and Methods

2.1 Cell Culturing

Cell line. Cell culture involves isolated interested cells and subsequently develops in vitro. Human monocyte-derived macrophage (MDM) was the main cell used in this project. Originally, buffy coats from a healthy donor were collected by the blood bank at St. Olavs hospital, Trondheim.

Besides the MDMs, Lilly Laboratories Cell-Monkey Kidney 2 (LLC-MK2) was additionally used for HMPV propagation.

Some cells involved in this project, included peripheral blood mononuclear cells (PBMC), Monocyte, Jurkat, A549, Caco-2, HT20, and Huh7.25.CD8, A549, HT29, SW480, and SW620, were not cultured. Only isolated RNA and cDNA were used. Those materials were isolated and stored in a freezer by senior Master and Ph.D. students.

Cell cultivation. Monocytes were obtained after isolating peripheral blood mononuclear cells (PBMC) by using Lymphoprep^{TM} (Serumwerk Bernburg AG) through gradient centrifugation. Afterward, isolated monocytes were seeded in either a 24-well plate (400 µl/well) or a 48-well plate (200 µl/well) with a required concentration of 1×10^7 cells/ml and cultured in RPMI-1640 (R8758, Sigma – Aldrich) with 10% A+, Glutamine, and Gentamycin. Non-adherent cells were vigorously washed away with pre-heated phosphate-buffered saline (PBS) after 90 min incubating. Monocytes were differentiated into monocyte-derived macrophages (MDM) in RPMI-1640 supplemented with 10% A+, and Glutamine, in the presence of macrophage colony-stimulating factor (M-CFS). The cells were cultivated in a 48-well cell culture plate in 5% CO_2 at 37°C. Fresh culture media were replenished every 3 days and were checked morphologically for differentiation. Cultured macrophages were then used for experiments, notably for treatment with HMPV, IFNs, siRNA, and/or ruxolitinib.

LLC-MK2, as abovementioned, was obtained from cryopreserved cells which were thawed and provided by a lab technician. They were cultured in Opti-MEM™ supplemented with 5% fetal bovine serum (FBS), Glutamine, and Gentamycin. Split sub-confluent cultures (70-80%) in a 75 cm^2 culture flask, with desired concentration 1.5×10^6 cells/mL using 0.25% trypsin/EDTA to detach the cells from the culture flask. The trypsinated cells were incubated for 5 min before they were resuspended in fresh growth media. The cells then were counted and split to get desired concentration so that was added into the new culture flask and incubated at 5% CO_2; 37 °C.

2.2 Cell Treatment

Transfection. siRNA transfection is a biological mechanism that intentionally deliveries the short interfering RNA (siRNAs) into the cultured cell to silence gene expression via the degradation of specific target mRNAs [61]. For gene silencing, specific siRNA reagents targeting IFNLR1, and All-stars negative control siRNA were used according to the siRNA double transfection protocols. In this experiment, siIFNLR1 was used to investigate whether the knockdown IFNLR1 had any effect on the signaling pathway of IFNs. The negative control was used to evaluate transfection efficiency.

siRNA including siIFNLR1 (IL28RA Silencer Select® Pre-designed siRNA - Ambion) and siAllStar Negative (Control siRNA - Thermo Fisher Scientific) were transfected into cells using Lipofectamine® RNAiMAX Reagent (Thermo Fisher Scientific) and pure Opti-MEM™ (Gibco). On the day before transfection, MDMs were cultured in a medium contained RPMI 1640 (R8758, Sigma – Aldrich), 10% A+, Glutamate, and M-CFS. The next day, either 320 µl (24-wells) or 160 µl (48-wells) medium was changed without M-CFS. The transfection mix including siRNA (IFNLR1 and negative control siAllStar), OptiMEM, and Lipofectamine was prepared beforehand and transferred into the plate, either 400µl (24-wells) or 200µl (48-wells), with a final concentration of 10nM and 20nM siRNA. After 24h of incubation at 37 °C, 5% CO_2, antibiotic-free growth medium was substituted with the transfection mix and continuously incubated for 1 day (under the same condition). The second transfection was achieved on the third day (repeated as the first transfection) whilst the last medium changed was done on the fourth day. After that, the cells were ready for further treatment. Depend on the type of experiment, the cells were either pre-treated IFNs or post-infected with HMPV or both.

RUX inhibition. Ruxolitinib or RUX is a JAK2/JAK1 inhibitor that blocks the inflammatory JAK-STAT signaling pathway. Ruxolitinib (Invivogen) was thawed on ice and spun down before being used. RUX with stock concentration was diluted with MDMs culture media (RPMI 1640, 10% A+, and Glutamate) to get the desired concentration of 5 µM and 10 µM in 400 µl/well (24 wells plate). Old culture medium was removed and replaced by master mixed RPMI 1640, 10% A+, Glutamate and RUX and incubated to 2 hours (37 °C, 5% CO_2) before applying a corresponding volume of 0.5 µg/ml IFN-λ1 or 250 U/ml IFN-β for 6 h (37 °C, 5% CO_2).

2.3 Infection

Virus propagation and isolation. HMPV strain was inoculated on LLC-MK2 cells with low multiplicities of infection of 0.01 (MOI) in Opti-MEM™ with 2 % fetal bovine serum (FBS) and 50 µg/mL trypsin at 37 °C, incubation time depend on the strands. Changing growth medium contained trypsin every 4 days. The virus was collected from cells and supernatant by freeze-thawing at -80°C, subsequently purification on a 20% sucrose solution and resuspension in cold Opti-MEM™ supplemented with 2% FBS.

Virus infection in vitro. MDM cells were seeded in 48 wells-plate for qRT-PCR with the desired concentration of 2×10^6 cells. On the day of infection, cells with confluence >70% were infected with HMPV at MOI of 1 at different timepoint. At the designated time points, cells and cell supernatants were collected for the following analysis.

In a distinct set of experiments, MDM cells were pretreated with 1 μg/ml of IFN-λ1 or 1000 U/ml IFN-β in 3 hoursand 24 hoursbefore the infection, followed by removal of the medium. Virus solution was preparedbeforehand including virus stock 1.65×10^6 PFU/ml and Opti-MEM™ with 2% FBS was added and incubated for 24 hoursand 48h at 37 °C, 5% CO_2 before harvesting.

2.4 Cell Lysis and Harvesting

Depend on the specific purpose, either immunoblotting or qPCR, an appropriate lysis buffer was added to the cell culture plate after removing media to lyse the cells and harvest its components.

Designed for RNA extraction, 1 mL lysis buffer RTL (QIAGEN) supplemented with 10 µl 2-Mercaptoethanol (Gibco). An amount of 350 µl lysis buffer was added per well and was resuspended. The cell suspension was transferred to the Eppendorf tube and stored at -20°C until extraction.

Regarding protein extraction, 1 mL 1% lysis buffer supplemented with 20 µl cOmplete™ Protease Inhibitor Cocktail (Roche), 10 µl phosphatase inhibitor cocktail (Sigma-Aldrich), and 10 µl phosphatase inhibitor cocktail 3 (Sigma-Aldrich). An amount of 60 µl lysis buffer was added per well. Adherent cells were scraped off the wells and transferred to the Eppendorf tube and stored at -20°C.

2.5 Immunoblotting

Western blotting. To detect the protein expression, samples were centrifuged at 4°C, 5000 rpm in 5 min to separate insoluble components and lysate. Lysate mixed with NuPage® LDS sample buffer and electrophoresed using NuPage® Bis-Tris gel 4–12% (Invitrogen) with running buffer containing MES, NuPAGE™ MOPS SDS Running Buffer (20X) (sodium dodecycl sulfate). The

cell extracts (~100 µg) were diluted in NuPAGE LDS (lithium dodecycl sulfate) sample buffer containing DTT (4X) (dithiothreitol). The samples, Seeblue MW (Invitrogen™, Thermo Fisher), and MagicMark™ XP Western Protein Standard were loaded into the wells, and the electrophoresis was run at 200V for 55 min. Samples were then blotted on a nitrocellulose membrane (Invitrogen) by Trans-Blot Turbo Transfer System (BIORAD) at 2.5 A and 25 V for 7 min. It was then incubated with anti-IFNLR1 (PA5-53583) (Invitrogen) overnight at 4 °C, followed by Goat Anti-Rabbit (IgG) at a 1:5000 dilution in Tris-buffered saline with 0.1% Tween® 20 Detergent (TBST). IFNLR1 protein was detected using ImageStudio with the settings: 700 and 800 channels.

2.6 Conventional PCR, gel electrophoresis

RNA extraction. To isolate the RNAs, lysates were transferred to RNeasy spin columns (Qiagen) and total RNAs was extracted by using the RNeasy® Mini kit (cat. No. 74104 and 74106) (Qiagen) in accordance with the manufacturer's protocol (Quick-StarProtocol) for animal cells, including adding the DNase to digest the trace of gDNA. In the final step, the purity and concentration of RNAs were measured by Thermo Scientific™ NanoDrop™ One Microvolume UV-Vis Spectrophotometer.

cDNA synthesis. Isolated RNAs were used to make cDNA by using qScript™ cDNA Synthesis Kit as the solution for RNA quantification using two steps qRT-PCR used according to the manufacturer's instructions. In general, an appropriate amount of RNAs and nucleasefree water were added together along with 4 µL qScript Reaction Mix (5X), and 1 µL qScript RT to get a final volume 20 µl per reaction. Appropriate controls reaction such as minus reverse transcriptase (-RT) and minus template control (-TC) are included in the experimental design. The settings for cDNA synthesis were programmed as follow: 22 °C for the first strand synthesis (5 min), 42 °C for reverse transcription (30 min), 85°C for deactivate reverse transcriptase (5 min), and hold at 4°C. cDNAs were kept undiluted for primer validation purpose; or diluted with autoclaved deionized water to get 2.5 ng/ml for gene analysis. These were kept in the freeze for further analysis with qRT-PCR.

Reverse transcription quantitative real-time PCR (RT-qPCR). Determine of genes expression by qRT-PCR was performed by using predesigned PerfeCTa® SYBR® Green FastMix®, ROX™. Briefly, a mastermix containing autoclaved deionized water, forward primer, reverse primer and SYBR Green FastMix (QuantaBio) were prepared and added to MicroAmp Fast Optical 96-Well Reaction Plate and later, the cDNA (3.75 ng in 1.5 µl) was added per each reaction. The Reaction Plate was sealed with MicroAmp Optical Adhesive Film and spun down (15 sec, 1000 rpm). The qPCR was done on a StepOnePlus Real-Time PCR instrument, with the settings 95 °C (20 sec) and 40 cycles of 95 °C (3 sec) and 60 °C (20 sec) each where the wanted gene was amplified by PCR using the primers are shown in Table 1. Target gene expression was normalized against either the glyceraldehyde 3-phosphate dehydrogenase (GAPDH) or TATA-Box Binding Protein (TBP) housekeeping gene. The result was analyzed by StepOne software.

Table 1 Primer pairs used in this study.

Gene target	Forward Primer (5' to 3')	Reverse Primer (5' to 3')
sIFNLR	TGGAGGTCCCAGGACTTTTCTG	CTGCAAGGTCCTTCTTCCATCTT
mIFNLR	CACGGGCCCTGGACTTTTCT	CTGCAAGGTCCTTCTTCCATCTT
OAS3	TGCAGCGGCAGCTTAAGAGA	TGAGCATCCAGCAGGTGGAA
CH25H	ATCACCACATACGTGGGCTTT	GTCAGGGTGGATCTTGTAGCG
Viperin	TGCTTTTGCTTAAGGAAGCTG	CAGGTATTCTCCCCGGTCTT
CXCL-10	GAAAGCAGTTAGCAAGGAAAGGT	GACATATACTCCATGTAGGGAAGTGA
IL-6	GATGAGTACAAAAGTCCTGATCCA	CTGCAGCCACTGGTTCTGT
HMPV	CATATAAGCATGCTATATTAAAAGAGTCTC	CCTATTTCTGCAGCATATTTGTAATCAG
GAPDH	GAAGGTGAAGGTCGGAGTC	GAAGATGGTGATGGGATTTC
TBP	GAGCCAAGAGTGAAGAACAGTC	GCTCCCCACCATATTCTGAATCT

Agarose Gel Electrophoresis. A helpful technique in determining whether contamination or unwanted replicons occurred in the negative control. If the bands for the negative control show products much smaller than the samples or positive control, it could be a primer dimer. But, if the band is the same or similar size as the positive control, it probably means there is some template contamination. The gel electrophoresis (75 V, 60 min) was done according to the Invitrogen™ 1 Kb Plus DNA Ladder protocol, with a 2% agarose gel (TBE) with 0.5X TBE buffer. DNA ladder and PCR products were diluted 1:10 with 10X BlueJuice Loading Buffer, stained with GelRed (30 min), and inspected in Bio-Rad Gel Doc.

Comparative Quantification. Method for comparative quantification is mostly applied in gene expression studies to determine the expression level of a gene of interest (GOI), for up- or down-regulation, in experimental samples relative to a control sample and normalize to a reference gene (also called housekeeping gene or endogenous control). The result for this changing represents as the fold-change or fold-difference. In this comparative method, a reference gene is treated as an error-control between samples when measuring gene expression due to its stability under external stimuli [62]. An arithmetic formula $2^{-\Delta\Delta C_T}$ is used to attain the result for relative fold gene expression with $\Delta\Delta C_T$ is the difference between the ΔC_T values of the experimental sample and the control sample. While the ΔC_T value refers to the subtraction of the average reference C_T value from the average GOI C_T value (average C_T corresponds to the average of the biological replicates) [63].

$\Delta C_T = C_T$ GOI $- C_T$ reference gene

$\Delta\Delta C_T = \Delta C_T$ experimental sample $- \Delta C_T$ control sample

Fold difference $= 2^{-\Delta\Delta C_T}$

The standard deviation of the $\Delta\Delta C_T$ value is the same as the one of ΔC_T value.

$$SD = \sqrt{SD_{GOI}^2 - SD_{ref}^2}$$

Statistics analysis. No statistical is available.

3 Result

3.1 Detection of IFNLR1 in MDMs

It is debated whether IFNLR1 is expressed in immune cells such as MDMs or not. To determine the presence of IFNLR1 in MDMs, we first analyzed the production of mRNA IFN-λ1 and -β in the cells in response to HMPV infection since the response to IFN-λ1 is controlled by the induction of the IFNLR1 expression. We infected the cells with HMPV at different timepoint 1, 3, 9, 15, 20, and 27 hours and mRNA expression of IFN-λ1, IFN-β, and HMPV was determined by RT-qPCR. As seen in Figure 9, HMPV infection induced an expression of IFNs at 1 hour but rose significantly after 9 hours. Unpredictably, IFN-λ1 was continuously up-regulated in the

MDMs at examination time points 15 and 20 hours, while IFN- β was induced to a lower extent and remained unchanged in the same duration. In corresponding with the vRNA, we found a steady upregulation of both IFN-λ1 and IFN-β in compromise with the increasing infection time, especially at the late time point 27 hours. Taken together, infection of MDMs with HMPV led to an induction of IFN-λ1 and IFN-β gene expression, though induction kinetics varied reproducibly between those two. Moreover, although both IFNs were induced against the viral infection, type III IFNs were favorably induced in response to HMPV infection.

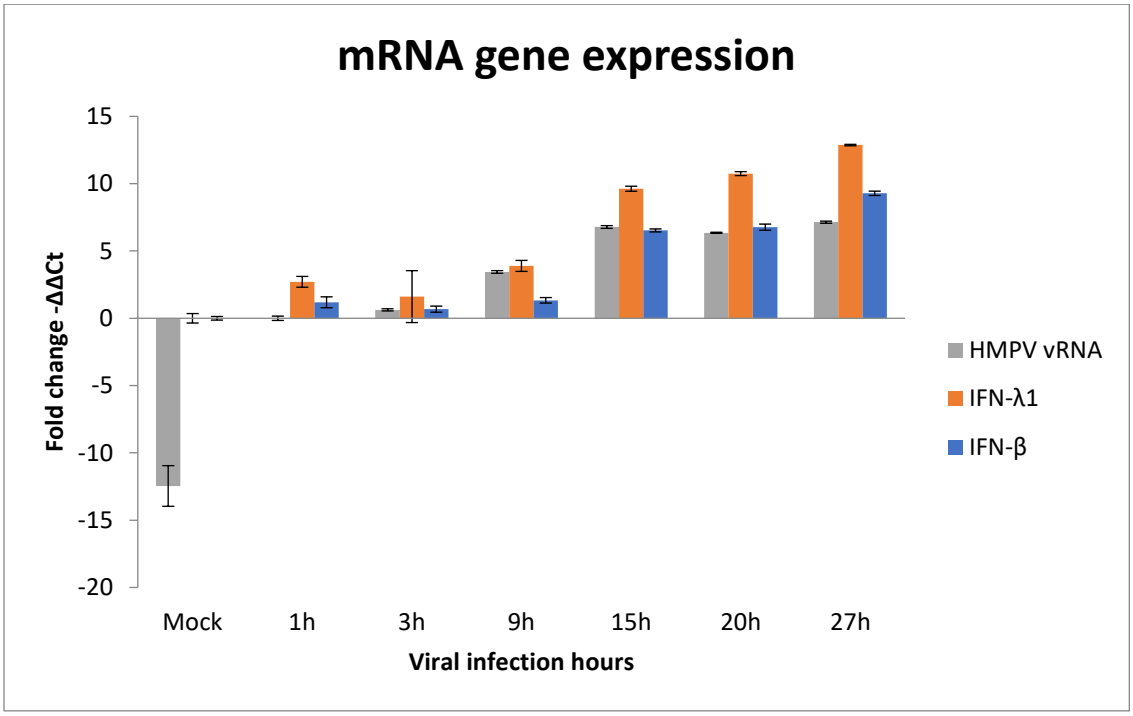

Figure 9 IFN-λ and IFN-β are induced in response to HMPV stimulation in MDMs. Total cellular RNA was extracted 1, 3, 9, 15, 20, and 27 h after viral challenge and gene expression was analyzed by using the delta-delta Ct method, the data shows a comparison of mRNA gene expression presented as the -ΔΔCt ± SD of three technical replicates. HMPV expression was normalized to HMPV 1 h. IFNs gene expression was normalized to CT

In contrast to the type I IFN receptor which is ubiquitous in most cell types, IFNLR1 is quite restricted and can mostly be found on epithelial cells [64]. To examine the expression of IFNLR1 in MDMs, we next analyzed the IFNLR1 protein levels in MDMs along with other cell types using the western blot technique. We expected to see the band showed IFNLR1 at approximately 55 kDa for two samples MDMs. As shown in Figure 10, all cell types showed a band with a size of approximately 55 kDa as expected and some auxiliary bands possibly equivalent to

alternatively spliced transcript IFNLR1 variants isoforms, except monocytes. These results suggest that MDMs were able to express IFNLR1 protein.

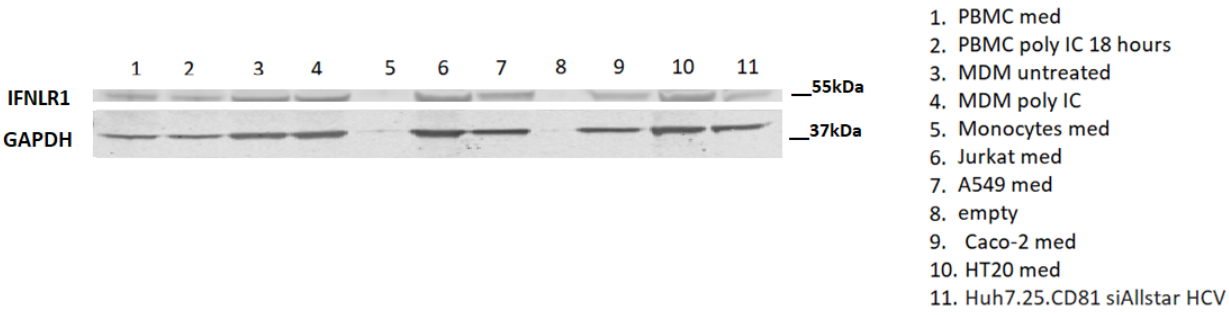

Figure 10 Protein expressions of IFNLR1 were analyzed in cell lysates of MDMs and different cell types include PBMCs, Monocytes, Jurkat, A549, Caco-2, HT20, and Huh7.25.CD81 using the western blot. The membrane was blotted against IFNLR1 (~55kDa). and loading control GAPDH (~37kDa).

We next determined expression of IFNLR1 mRNA in different cell types in human cells had been mentioned, including sIFNLR1 and mIFNLR1 [33-35], we wanted to determine if MDMs express IFNLR1 as seen on epithelial cell lines. We then used qRT-PCR to analyze the transcription level of the sIFNLR1 and mIFNLR1 on 8 different cell types: A549 (as the control), Jurkat, PBMC, HT29, Huh7, SW480, SW620, and MDMs. These cells can be divided into two groups: originated from blood (PBMC, MDM, Jurkat) and epithelial cells (A549, HT29, Huh7, SW480, SW620).

We used primer sequences for human sIFNLR1 and mIFNLR2 in this experiment came from Deanna et al. [65]. The efficiency of each primer set for RT-qPCR was determined to be 110% and 95% respectively (Supplementary Figure 1A). The PCR products were ran on an agarose gel to confirm that products of the expected size were detected and no off-target amplification products if they showed multiple peaks (Supplementary Figure 1B).

We next assessed the presence of IFNLR1s on these cells by quantitative RT-PCR. We first opted to normalize to a reference gene GAPDH. Subsequently, to reconfirm the result, two more qPCRs were performed but with a different approach, in which the samples were normalized to the geometric mean of two reference genes, GAPDH/TBP and β-actin/TBP as described [65] (Supplementary Figure 2A and B). Take a note that in these two attempts, the A549 medium was replaced by A549 HMPV 18h due to the shortage of material. However, the adjustment did not make any significant change in C_T value so that it was valid to use.

Surprisingly, by using qRT-PCR and GAPDH as reference gene, we found that among the other samples, MDMs had the highest expression of mIFNLR1 transcript (27-fold), followed by PBMC (24-fold) (Figure 11). HT29, Huh7, and SW480 induced a smaller amount of mIFNLR1 mRNA while SW620 barely expressed the level of the mRNA transcript. The same pattern was also observed in the sIFNLR1 level, with an exception has occurred in PBMCs and MDMs, such that the former induced 20 times higher mRNA splice variant transcript than MDMs. Additionally, it was unexpected that we observed a down-regulation expression levels for sIFNL1 and mIFNLR1 mRNA in Jurkat subjects, compared with A549 - the control. Since this was contradict with result from immunoblotting (Figure 10) that showed protein expression for Jurkat cells, the band also wider in comparison with A549 next to it.

More intriguingly, those samples derived from blood excluding MDMs had sIFNLR1 dominantly expressed, whilst samples originated from epithelial had less sIFNLR1 but instead governed by mIFNLR1 (Figure 11). Consistent with our results from the qRT-PCR, samples originated from blood expressed predominantly the IFNLR1s compared to other epithelial samples, may suggesting high IFNs type III responsiveness of MDMs.

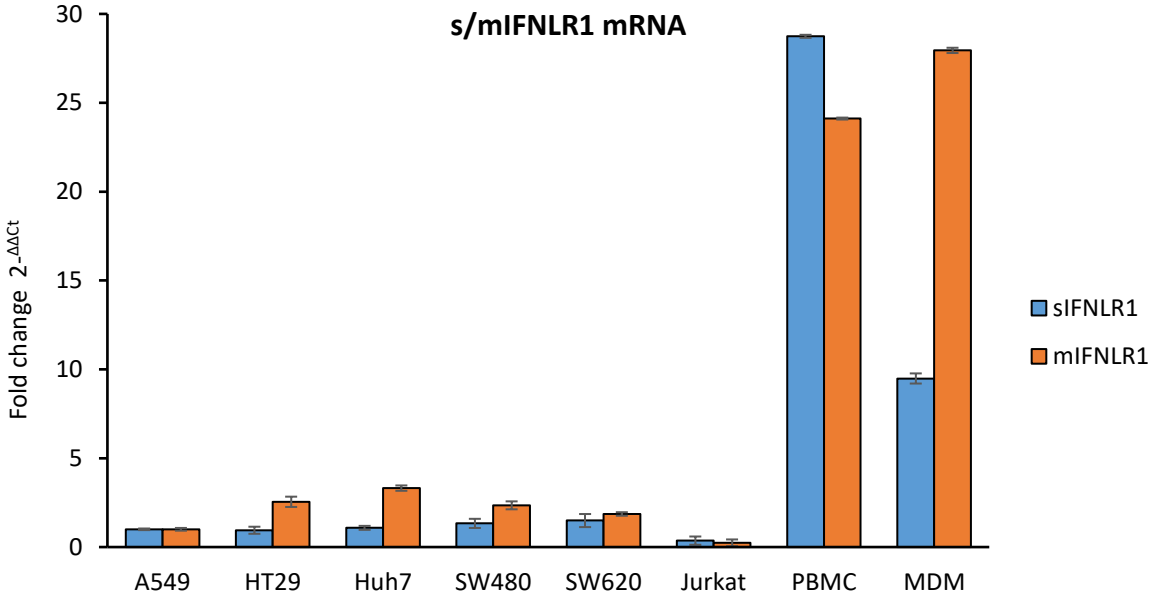

Figure 11 Expression of IFNLR1 variant (sIFNLR1 and mIFNLR1) on different cell types. RT-qPCR was used to determine the relative expression of mIFNLR1 and sIFNLR1 forms of IFNLR1 with normalization to the reference gene GAPDH. The data showed for A549, Jurkat, PBMC, HT29, Huh7, SW480, SW620, and MDM. Relative expression values were calculated normalized to A549 (control). Data shows $2^{-\Delta\Delta Ct} \pm SD$ (n = 3). The data came from one separate experiment.

3.2 Type I and III IFNs Attenuate HMPV Replication in MDMs

To investigate the antiviral activity of type I and III IFNs in response to viral replication in vitro, transcription levels of vRNA were measured in MDMs pre-stimulated with IFN-λ1 (1 μg/ml) and IFN-β (1000 U/ml) for 3 or 24 hours before infection. After the incubation time, the cells were intently infected with HMPV with MOI of 1 for 24 or 48 hours. Also, cells were treated by HMPV for 1h

In assessing the kinetics of HMPV replication, Figure 12A exhibited significantly more vRNA load in cells increased considerably after two days of infection, triple the amount of viral load from 24 to 48 hours. As showed in Figure 12B, in the first 24 hours post-infection, a moderate reduction of viral gene expression (7 folds) was seen in the cells pre-stimulated with IFN-β in 3 hours. Though in the same treatment, no change was observed in IFN-λ1 treated samples, but it halted the replication. Surprisingly, extended IFNs incubation for up to 24 hours failed to decrease viral mRNAs expression but instead promoted the viral expression 12-fold by IFN-λ1 and 6-fold by IFN-β treatment over the non-treatment samples (HMPV 24h). Only 3h treatment with IFN-β was capable to restrict the viral replication after 24 hours.

After 48 hours (Figure 12C), the production of vRNA in response to IFNs treatment was reduced overall, and considerably decrease was observed after 24 hours cytokines pre-treatment regardless of IFN-λ1 (52-fold) or IFN-β (78-fold). By 3 hours IFNs pre-treatment, a decrease in the production of vRNA by viruses was observed in both types I and III IFNs, though HMPV was strongly inhibited by IFN-λ1, as compared with IFN-β. Taken together, these data suggest that 24 hours pre-treatment with both types I and III IFNs can efficiently hinder the viral replication after 48-h post-infection. Type III IFN responsiveness to HMPV infection appeared to be delayed by 1 day to worked in relative to the type I IFNs (Figure 12B and C).

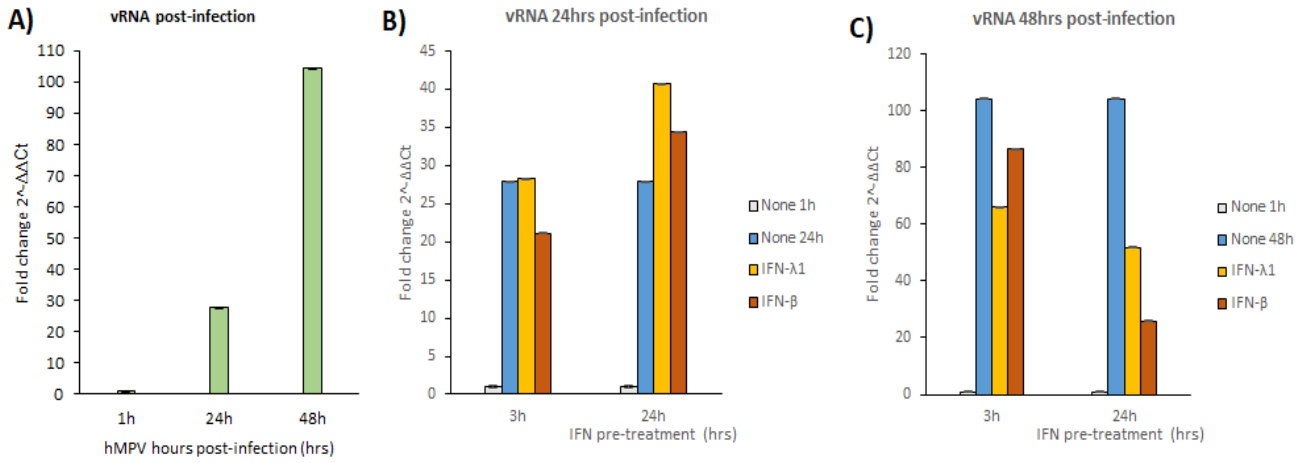

Figure 12 The presence of IFNs type I and III in MDM infected HMPV-infected samples interfere with viral replication. The expression of vRNA in HMPV-infected MDM cells was quantified by qRT-PCR and normalized to GAPDH. Cells were infected with HMPV at MOIs of 1. A) vRNA was determined at 1, 24, 48 hours after infection. Cells were pre-treated with IFN-λ1 (1 μg/ml) and with IFN-β (1000 U/ml) in 3 and 24 h, then were harvested and assessed after infection in B) 24 and C) 48 h. The data were from a single experiment that was representative of three biological replicates. Fold-change values were calculated relative to HMPV 1h (control). Data shows $2^{-\Delta\Delta Ct} \pm SD$ *(n = 3).*

Next, we examined HMPV-induced proinflammatory chemokine and antiviral protein responses, by measuring changes in the expression of Viperin and CXCL-10 mRNA levels in MDMs that had been pre-treated IFN-λ1 or IFN-β prior to HMPV infection in order to determine whether IFNs has an effect on viral infection.

Primer target human CXCL-10 was from Roche. The efficiency of primer set for RT-qPCR was determined to be 99% (Supplementary Figure 3A). The PCR products ran on an agarose gel to confirm that products of the expected size were detected and no off-target amplification products if they showed multiple peaks (Supplementary Figure 1B).

We found that HMPV replication were accompanied by significant increases in Viperin and CXCL-10 gene expression at the mRNA level (Figure 13A). Viperin was absent in the first hour but the expression significantly up-regulated in the first day (470-fold), and reach the highest amount on the second day that was 2.5 times the first 24 hours (1196-folds). CXCL-10 on the other hand, exhibited an opposite trend even though its mRNA reached maximal levels (552-fold) at 24 hours infection then declined.

We also analyzed whether the magnitude of ISG expression (CXCL-10 and Viperin) was dependent on the duration of initial IFNs treatment to which MDMs were exposed. There was a significant elevation of Viperin, regardless of the type of IFNs, were observed at both 24 hours and 48 hours post-infection with the peak of the ISGs product was seen at 48 hours post-infection in MDM cells received the IFNs pre-treatment in 3 hours (2100-fold in response to IFN-λ1 and 3900-fold in response to IFN-β). Unexpectedly, prolonged exposure time with IFNs can help in upregulation of the IFN-stimulated genes after 24 hours of infection but not after that, mRNA levels were reduced after 48 hours (Figure 13B and C).

On the other hand, CXCL-10 mRNA expression decreased with HMPV infection time and with pre-IFNs treatment time (Figure 13D and E). A favored type III IFN response over type I IFN has been observed if we prolonged IFNs-treatment time, which upregulated CXCL-10 at the transcriptional level at both 24- and 48-hours post-infection. However, upon treatment with IFN-β in 3 hours before exposure to HMPV for 48 hours, the magnitude of CXCL-10 mRNA expression reached the highest (509-fold) among the other samples (Figure 13E). Similar results were observed for Viperin as abovementioned.

Altogether, our results suggest that both type I and type III IFNs may affect Viperin and CXCL-10 in response to HMPV infection, but their mRNA expression depended on the duration of IFNs pre-treatment. This means that if increasing IFN pre-treatment time in accommodate with infection time, mRNA of Viperin will increase whereas CXCL10 will decrease. In addition, even though type III IFNs displayed a low magnitude in gene induction against viral infection than type I IFN, but during first 24 hours infection they maximize mRNA induction earlier compared to type I IFN, (48 hours) (Figure 13).

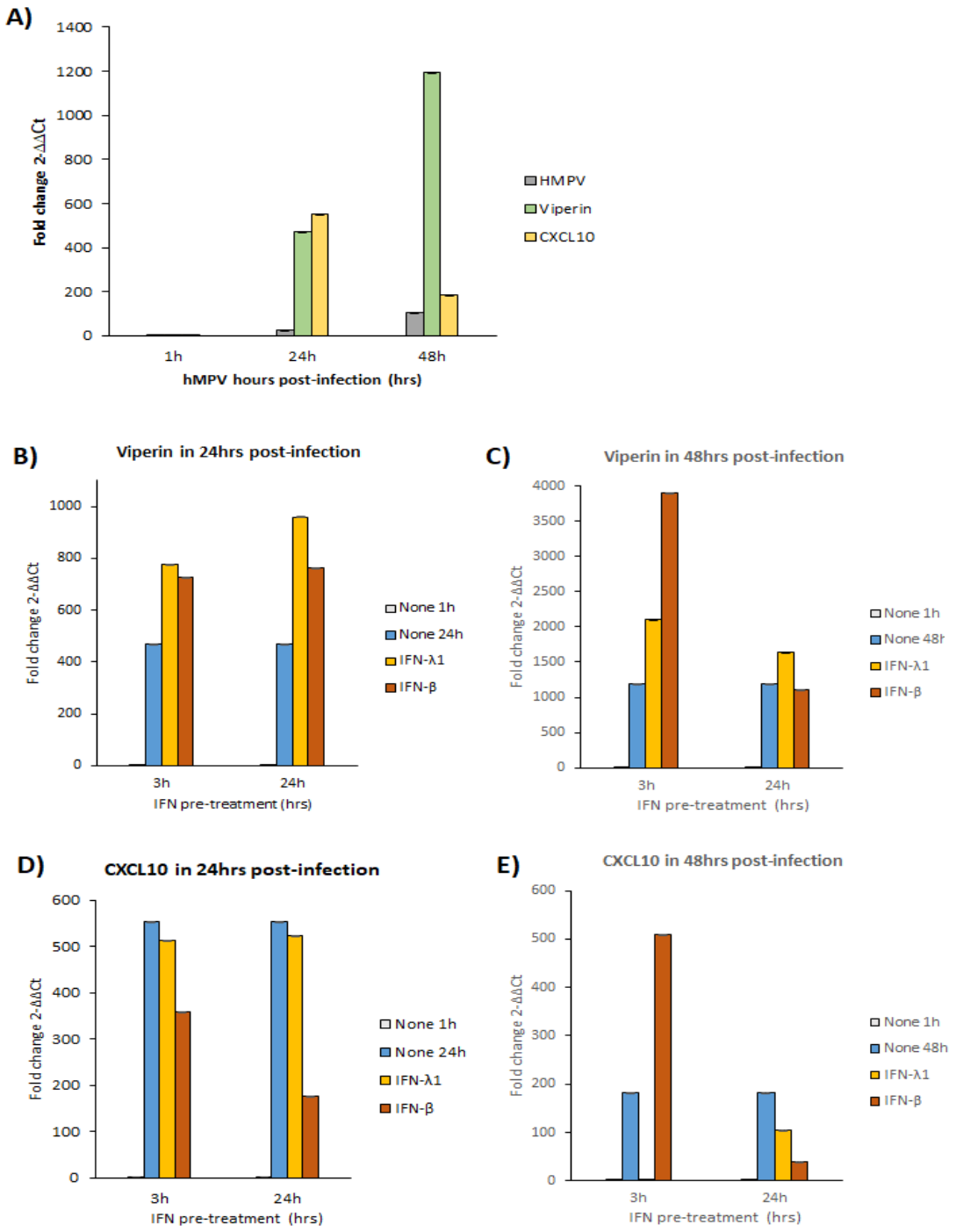

Figure 13 Infection of human MDM cells with HMPV induced Viperin and CXCL-10 mRNA in a time-dependent manner. Cells were infected with HMPV at MOIs of 1. Viperin and CXCL-10 mRNA was determined A) at 1, 24, 48 hours after infection. Cells were pre-treated with either IFN-λ1 (1 μg/ml) or IFN-β (1000 U/ml) in 3 and 24 h, prior to harvest and analyze by qRT-PCR and normalized to housekeeper gene GAPDH after infection in B) D) 24 and C) E) 48 h. The data were from a single experiment that was representative of three biological replicates. Fold-change values were calculated relative to HMPV 1h (control). Data shows 2-ΔΔCt ± SD (n = 3).

3.3 Type I and III IFNs in Induction of ISGs

To determine if type I and III IFN signaling in the regulation of ISGs gene expression in MDMs is different as had been reported in human lung cells [66], and colon organoids [67]. We assessed the ISGs expression of both IFNs by a time-course experiment. MDMs from three donors were stimulated with either IFN-λ1 (0.5 μg/mL) or IFN-β (250 U/mL) in the duration of 2, 4, 6, 8, 10, and 12 hours (Figure 14). After each time point, the cells were harvested, and the transcription level of Viperin, CXCL-10, and IL-6 was measured by real-time qRT-PCR.

The IFN mediated induction of two well-defined anti-viral ISGs Viperin and CXCL-10 were analyzed. Viperin was detectable in cells at 2 h, and yield the highest expression at 10 ~ 12 hours depend on the donor (Figure 14A, B and C). However, treatment with IFN-β greatly enhances the production of antiviral response in relative levels of mRNA induction despite IFN-λ1 showed similar upregulation kinetics.

Besides the finding that induction of CXCL-10 was significantly increased upon treatment with IFN-β, as had been mentioned in Forero et al. [68], the treatment with IFN-λ1 likewise succeeded to promote the induction of CXCL-10 mRNA. Even though, both type I and III IFNs triggered the production of CXCL-10 at 2 h, the kinetic for its transcription to reach its maximum induction was different, at 6 ~ 8 hours and 8 ~ 10 hours incubation respectively (Figure 14D, E and F). In general, the mRNA transcripts for the IFN-inducible gene Viperin and chemokine CXCL-10 were significantly increased following the treatment with either type I or type III IFN.

We then opted to examine IL-6, a multifunctional cytokine [69, 70], which is identified as a key modulator of T-cell function [71] and subsequently, can connect to IFN-λ1 – a bridge between innate and adaptive immunity [70]. Macrophages in response to PAMPs released the proinflammatory cytokine IL-6 to mediate the innate immune response [70]. The kinetics of IL-6 production was detectable in response to IFN-λ1 within 2 hours of culture, but very low extent. Such a minor signal was significantly apparent only after 4 h of cell incubation, and subsequently reached maximized at 8 hours stimuli. Under the same experimental conditions, IFN-β began to have its effects at 2 hours and reach the highest secretion at 6 hours (Figure 14G, H and I).

CH25H has an essential role in controlling lipid metabolism, gene expression, and immune activation [55]. Recent studies have described that IFN type I can regulate CH25H expression in murine macrophages [54, 55, 72]. To expand these finding on human MDMs, we measured the transcription levels of CH25H in human MDMs pre-stimulated with IFN-λ1 and IFN-β for different length of time. Of note, among abovementioned ISGs, CH25H is the first interferon stimulate gene that maximal production early in MDMs (Figure 15). Both IFN-λ1 and IFN-β appeared to be able to induce CH25H expression in MDMs and the induction occurred rapidly and highest after 2 hours of pre-treatment, followed by a decline in mRNA expression coupled with extended treatment time for both types of IFNs. Even though a similar expression pattern was observed in both IFN-λ1 and IFN-β, the latter exhibited a significant up-regulation of CH25H transcription ∼2 times in comparison with the former, which expressed less extent. Moreover, IFN-λ1 mediated treatment had short duration in stimulate CH25H as started to decline after 10 hours IFN treatment (Figure 15A). However, if we compare with CXCL-10 induction, (a well-known ISG controls) which were highly induced, the changed was dependent on the type of IFNs stimulation. More specifically, upon IFN-λ1 treatment, CH25H mRNA expression levels surged up (90-fold) higher than CXCL-10 in the first 2 hours, then dropped down to around 10-fold and started to diminish after that. On the other hand, CH25H mRNA expression levels reached maximum at ∼1000-fold (2 hours) when stimulated with IFN-β, 10 times as witnessed in IFN-λ1. Still the change was minor as compared with the induction of CXCL-10 (5000-fold). Our result indicated that with this concentration of 0.5 μg/mL IFN-λ1 and 250 U/mL, the IFNs initiate induction of the CH25H mRNA expression in MDMs.

Taken together, these data illustrate that type I IFN ultimately gave the highest induction of all ISGs analyzed compared to type III IFNs. The variation in the ISGs expression magnitude was independent of IFN treatment time except for Viperin. Separate gene expression analysis has suggested that most of the genes significantly induced by type I IFN were also induced by type III IFN, even though type III requires more time to establish an antiviral state. The duration to reach the peak varied for each donor.

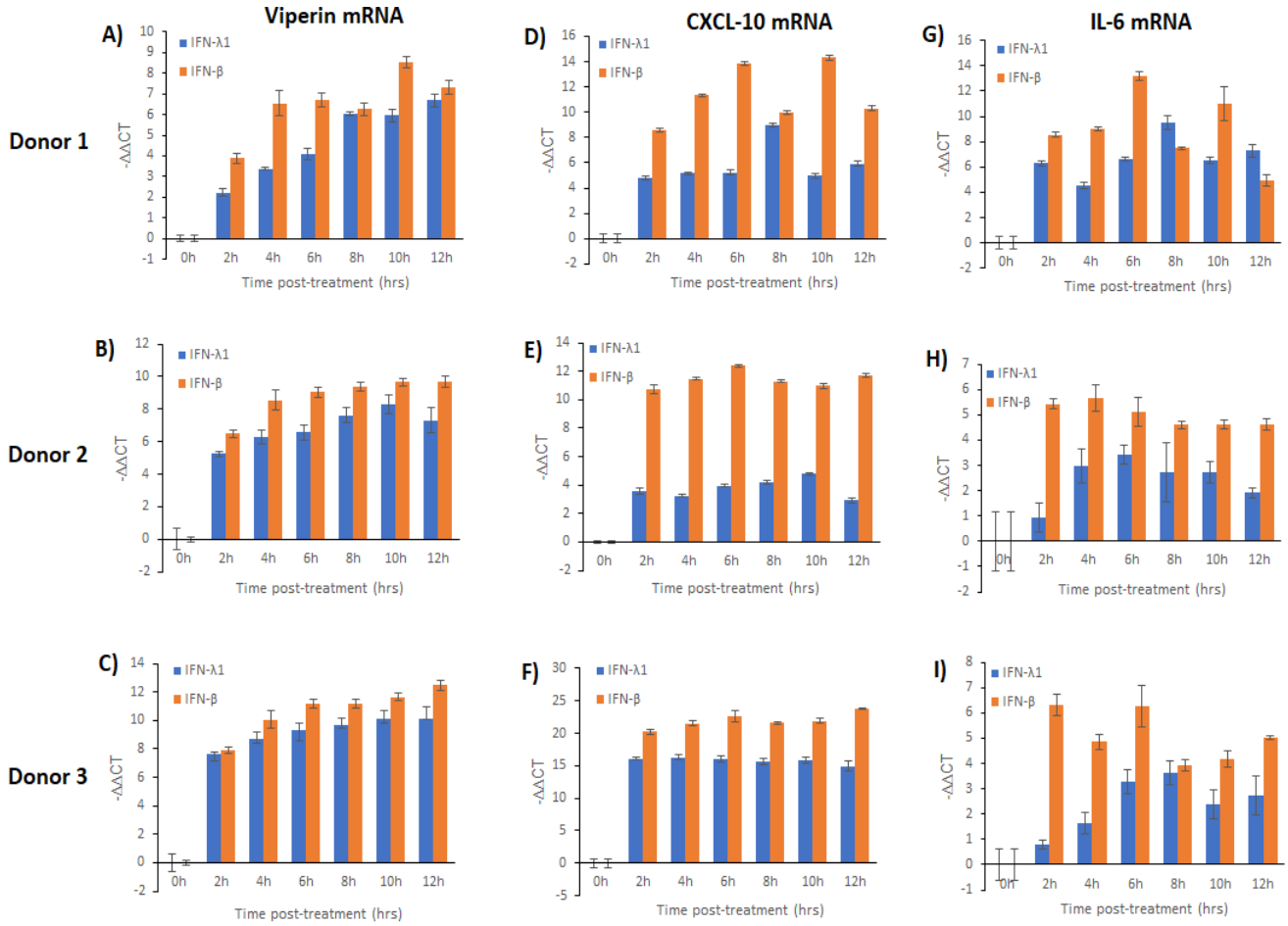

Figure 14 ISGs and cytokine expression regulation upon the IFNs pre-treatment. MDMs were isolated from the peripheral blood of healthy donors and were left treated with 0.5 μg/mL IFN-λ1 and 250 U/mL IFN-β for consecutive even hours, up to 12 hours to evaluate: A) CH25H, B) CXCL-10, C) Viperin and D) IL-6 mRNA expression, by RT-qPCR. Gene expression data (-ΔΔCt ± SD, three replicates, three donors) was normalized to GAPDH.

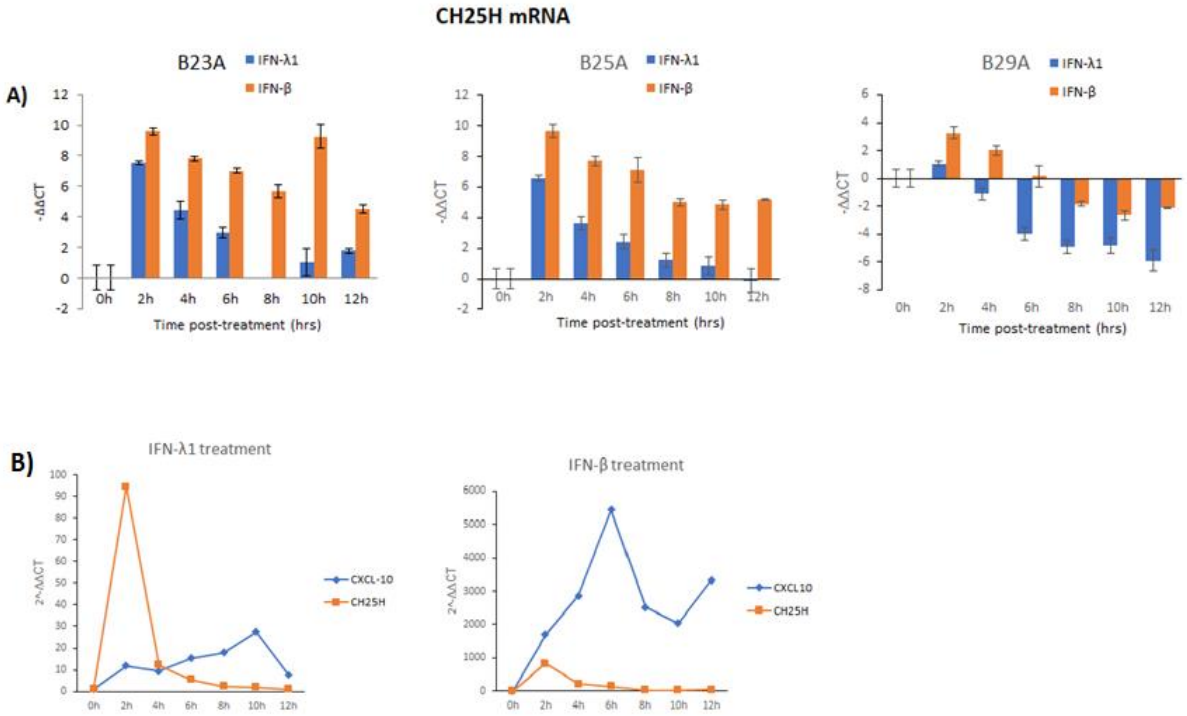

Figure 15 CH25H expression regulation upon the IFNs pre-treatment. A) MDMs were isolated from the peripheral blood of healthy donors and were left treated with 0.5 μg/mL IFN-λ1 and 250 U/mL IFN-β for consecutive even hours, up to 12 hours to evaluate by RT-qPCR. Gene expression data (-ΔΔCt ± SD, three replicates, three donors) was normalized to GAPDH. B) Gene expression of CH25H in comparable with CXCL-10, as a ISG control. Two separately qPCR analyze. Data taken from the same batch. Gene expression data ($2^{-\Delta\Delta Ct}$ ± SD, three replicates, 1 donors) was normalized to GAPDH.

3.4 The Impact of siIFNLR1 Transfection on IFN-treated or HMPV-Infected MDMs

To explore the importance of IFNLR1 to ISGs induction, we investigated the induction of ISGs mRNA in IFNLR1 deficiency by using siRNA transfection to knockdown IFNLR1 in vitro. In order to determine the suitable siRNA concentration, MDMs were transfected with either 10 nM or 20 nM and harvested after 4 days of double-transfection transfection. In the analysis of the siIFNLR1 target gene knockdown efficiency, qRT-PCR was used to analysis of the knockdown at the mRNA level using the ΔΔCT method. Data obtained from RT-qPCR analysis of mRNA levels following siRNA knockdown was described in Figure 16. Successful knockdown of IFNLR1 was observed by the reduced levels of mRNA. The knock down effects was calculated by comparing mRNA expression in siIFNLR1-treated samples to non-targeting control cells. The

level of knockdown achieved in 10 nM were 65.2% for sIFNLR and 77.9% for mIFNLR1. The same pattern was also observed in 20 nM siRNA concentration but 10% more efficiency. Taken together, this indicated that a minimum concentration of 10nM siRNA is suitable for the knockdown of the IFNLR1.

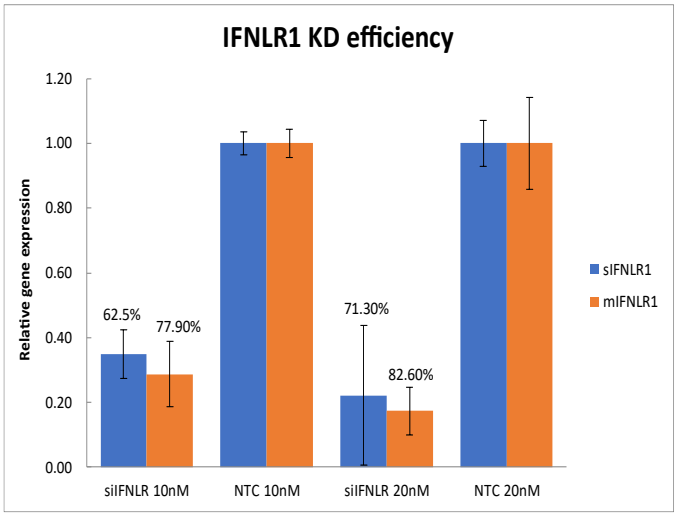

Figure 16 siRNA-mediated silencing of siIFNLR1 was measured using a ΔΔC_q method to verify relative gene expression from RT-qPCR data with GAPDH as an endogenous reference gene. MDMs were treated with siRNA to IFNLR1, and with a non-silencing control siRNA (siAllStar) at either 10 or 20 nM and RNA harvested at 4 days post-double transfection. The cells demonstrated siRNA dose-dependent knockdown of IFNLR1, with mRNA decreased by 62.5%, 71.3% (sIFNLR1) and 77.9%, 82.6% (mIFNLR) when cells were treated with 10 and 20 nM, respectively.

To examine the effect of IFNLR1 knockdown on the replication of the virus, after siRNA transfection a dose of HMPV MOI 1 was used to infect siIFNLR1 or siAllStar-treated MDMs for 24 hours and 48 hours. The vRNA expression level was measured by RT-qPCR. Figure 17A shows that when IFNLR1 was knocked down, cells appeared to be more susceptible to HMPV infection so that vRNA increased considerably higher than in mock-transfected cells. These data suggested that IFNLR1 is functionally in antiviral defense against HMPV infection of MDMs.

Next, we assessed the impact of siIFNLR1 transfection on ISGs induction by IFN or HMPV stimulation. In a previous time-course experiment, we already examined the IFN-inducible genes produced by human MDMs in response to IFN-λ1 and IFN-β (Figure 14) and found that 6 hours and 10 hours were optimal for induction Viperin, CXCL-10, and IL-6. In this study, MDMs after received double transfection with siIFNLR1, cells were stimulated with either 0.5 μg/mL IFN-λ1 or 250 U/mL IFN-β for 6 hours and 10 hours prior to analysis of mRNA for the interested IGSs

(Viperin, CXCL-10) and the cytokine IL-6 by qPCR. For HMPV infection, 24- and 48-hours was used. We expected little or no ISGs expression in the samples that received IFN-λ1 treatment.

type III IFN signaling activates an antiviral response by an alternative pathway.

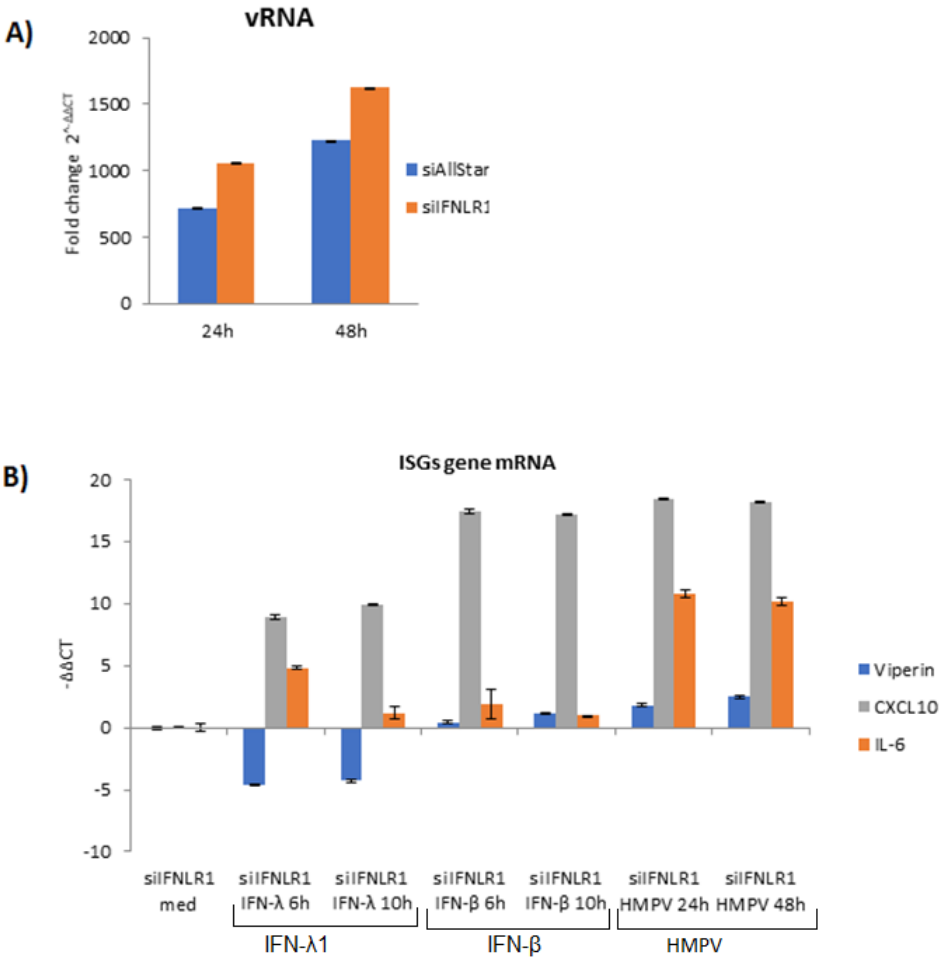

Figure 17B showed knockdown of IFNLR1 impaired the induction of Viperin in the IFN-λ1 stimulated cells relative to untreated cells (culture media only). In contrast, under the same IFNLR1 knock-out condition, MDMs still up-regulated Viperin mRNA if the cells received IFN-β treatment, still, it was nearly visible until 10 hours. We found that infection of MDMs with hMPV, at an MOI of 1, caused a moderate increase in Viperin mRNA compared to IFNs treated cells.

For three types of stimulation, the mRNA expression of CXCL-10 did not differ significantly between two timepoints. Notably, with the presence of IFN-λ1, the levels of CXCL-10 expression increased when prolonged the treatment's hours as opposed to the other two (IFN-β and HMPV), even though this was a minor increase.

Surprisingly, cytokines such as CXCL-10 and IL-6 demonstrated high levels of secretion even in the absence of IFNLR1. This means that MDMs can secrete those two cytokines in a type III-independent manner which indicated the presence of alternate production pathways. Moreover, the IL-6 mRNA induced by type III was higher than type I treated cells might suggest IFN-λ1 appears to play an important role in IL-6 induction.

In general, the knockout of IFNLR1 might have a great impact on the expression of ISGs particularly Viperin for both IFNs treatment and viral infection. An unexpected result was observed in the upregulation of pro-inflammation cytokine CXCL-10 and IL-6, which might suggest type III IFN signaling activates an antiviral response by an alternative pathway.

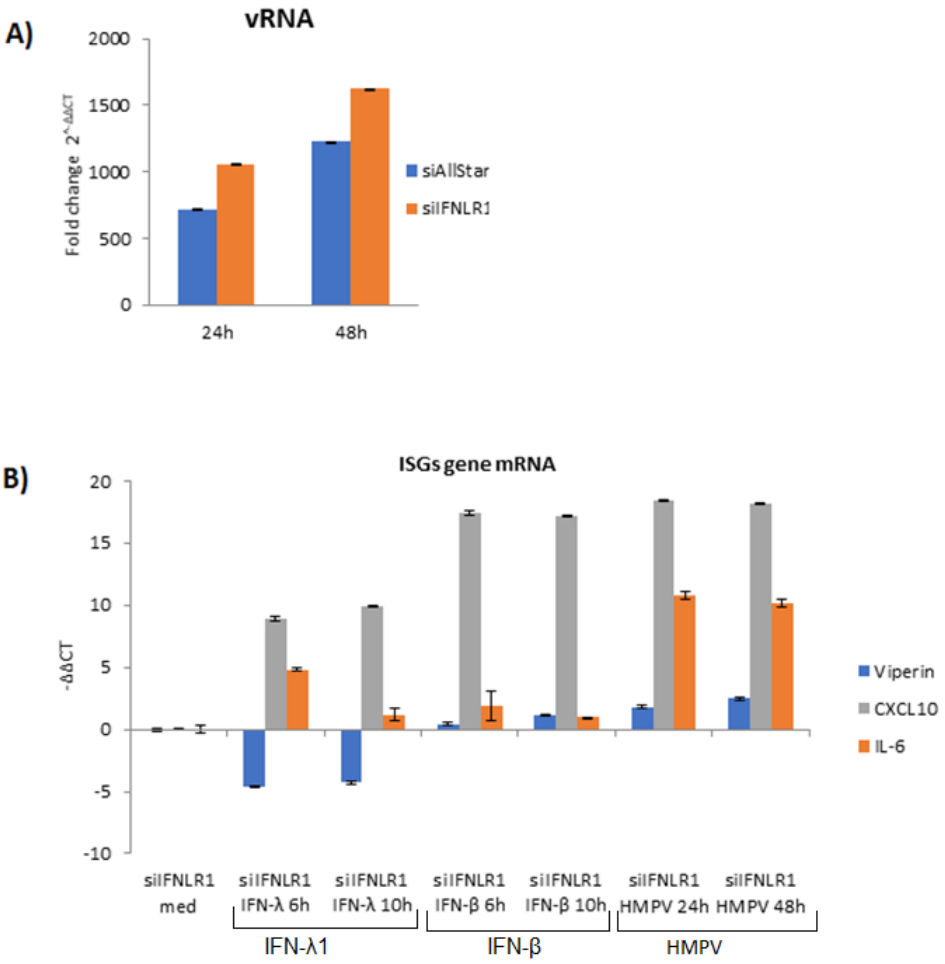

Figure 17 siRNA-mediated knockdown of IFNLR1 mRNA in human MDMs. Cells were transfected with a concentration of 10 nM of siIFNLR1 for 2 hours. After transfection A) MDMs were infected with HMPV at a MOI 1 for either 24 h or 48 h. Cells were harvested for vRNA expression. Gene expression data (2-ΔΔCt ± SD, three replicates) was normalized to GAPDH. B) MDMs were stimulated with either 0.5 µg/mL IFN-λ1 or 250 U/mL IFN-β for 6 hours and 10 hours and total RNA was extracted for qRT-PCR analysis of Viperin, CXCL-10 and IL-6. Gene expression data (-ΔΔCt ± SD, three replicates) was normalized to GAPDH.

3.5 Ruxolitinib Down Regulates ISGs and Block the Pro-Inflammatory Cytokine IL-6

To activate the heterotrimeric transcription factor of the ISGF3 complex, downstream signaling of both type I and III IFNs must occur via the JAK -STAT pathway. Here, we examined whether the JAK1/2 inhibitor ruxolitinib had affected IFN-induced ISGs or IL-6. MDMs were pre-treated with either 5 µM or 10 µM RUX inhibitor for 2 hours, followed by 6 hours treatment with 0.5 µg/mL IFN-λ1 or 250 U/mL IFN-β. These 5 µM or 10 µM concentration of ruxolitinib did not affect viability of macrophages in response to a 2-hours exposure as evaluated by morphology of

the cells. The 6-hours of IFNs post-treatment was chosen for this study because it was the average time where the ISG gene showed a moderate induction (Figure 14).

As expected, treatment with IFN-λ1 will induce Viperin, CXCL-10, CH25H and IL-6, but were significantly downregulated by the action of ruxolitinib at both concentrations 5 and 10 μM (Figure 18, half to the left side).

In contrast, in IFN-β-treated samples, 5 μM ruxolitinib did not completely inhibit mRNA expression of reference ISGs such as Viperin, CXCL-10 and CH25H. Respectively, 23%, 42% and 86% of these genes has impaired mRNA expression in ruxolitinib-treated MDMs as opposed to untreated counterparts (Figure 18, half to the right side). However, when increasing the concentration of ruxolitinib up to 10 μM, it affected mRNA cytokine induction with a total of ∼40% relative to what was observed at 5 μM ruxolitinib. Most of the targeted genes being suppressed (67% for Viperin and 86% for CXCL-10) (Figure 18A and B, half to the right side). No up-regulation was observed in CH25H and IL-6 in the pre-treatment 10 μM ruxolitinib, resulted in considerable down-regulation of mRNA (Figure 18C and D, half to the right side).

These data suggest that in human MDMs, IFN-λ1 and IFN-β induces ISGs and IL-6 via JAK/STAT dependent pathway. Moreover, this could point to a functional IFNLR1 in human MDMs. Ruxolitinib completely blocked IFN-λ-induced Viperin, CXCL-10, CH25H and IL-6. For IFN-β, RUX at 5 μM only inhibit cytokine IL-6, while 10 μM RUX partly blocked IFN-β induction of these ISGs (Viperin and CXCL-10) (Figure 18).

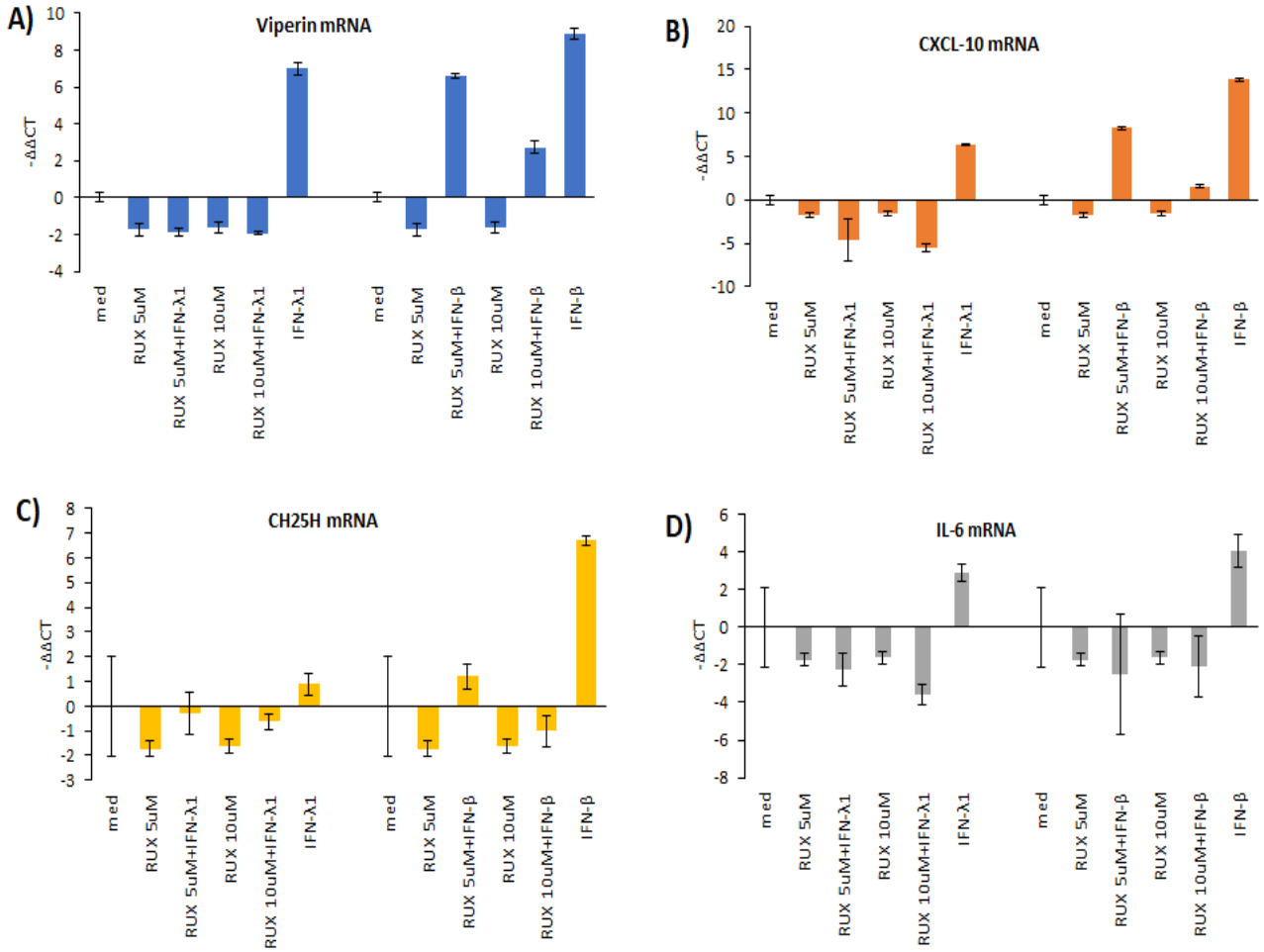

Figure 18 Ruxolitinib downregulates the IFN signaling pathway in human macrophages. MDMs were either untreated (control), exposed to 5 μM or 10 μM Ruxolitinib for 2 h, then incubated with either IFN-λ1 (0.5 μg/mL) or IFN-β (250 U/mL) in 6 h. mRNA expression of interferon-stimulated genes (ISGs) and cytokine include A) Viperin, B) CXCL-10 C) CH25H and D) IL-6 were determined by RT-qPCR. Data are expressed as mRNA expression fold change compared to untreated MDMs. Gene expression data (-ΔΔCt ± SD, three replicates) was normalized to GAPDH.

4 Discussion

In recent years, the specific roles of type III IFNs has become an interested subject for many studies, especially its effect in epithelial cells. In contrast, very little is known about the effects of type III IFNs on immune cells and it IFN-λ1 are able to affect immune cell, but just a few in immune cells since they are known to be restricted to IFN-λ responsiveness [73, 74]. In this study, we examined the role of IFN type I and type III in human MDMs, which is together with lung epithelial cells are the first line of defense during HMPV infection [75].

4.1 Detection of IFNLR1 in MDMs

In general, virus infection results in the release of IFNs which acts as autocrine or paracrine signaling binding their ubiquitous IFNR [40, 41]. Thus, the response to IFNs may be controlled by the induction of the receptor expression. Understand this, we first determined the expression of IFNs in the MDMs infected with HMPV at different hours. MDMs respond early to the infection by inducing IFNs to induce an antiviral response.

Indeed, the result indicates that both IFN-λ1 and IFN-β mRNA are up-regulated by MDMs shortly after the first hour post-infection, but differ in the magnitude, where IFN-λ1 levels were much greater than IFN-β levels. This demonstrate that IFN-λ1 is the predominant IFN produced in response to HMPV infection in human MDMs. A similar pattern has been observed in epithelial and dendritic cells but infected with Influenza virus [40].

After that, we determined the IFNLR1 via immunoblotting, our result indeed visualized IFNLR1 appeared in MDMs and other cell lines but no expression on monocytes. The results agreed with the claims of Liu et al. [76] that IFNLR1 is not expressed by human primary monocytes, but monocyte-derived macrophages. We additionally show that PBMC cells express significant amounts of IFNLR1 (both the soluble and membrane-bound receptor) in comparison with epithelial cells. To our understanding this is the first time MDMs was used in addition with other lines to compare side by side. Take a note that the expression level might vary among donors. However, we do not know if the high expression of IFNLR1 will be proportional to the sensitivity toward IFN-λ1 or the other way round. This had been mentioned in Lafsa et al. [34] with two opposite cases, that the first case was lymphoid tissues responded to IFN-λ quite weak even their IFNLR1 expression was significantly high. The second one was in B cells in which three-fold higher IFNLR1 compared to in keratinocytes, which were exhibited highest response to IFN-λ. Still, there remain some questions to be answered in further studies such as does the ratio sIFNLR1/mIFNLR1 affect the IFN-λ1 responsiveness? What is the mechanism behind it?

4.2 Type I and III IFNs Attenuate HMPV Replication in MDMs

It is largely unknown if type III IFNs can affect human immune cells. In previous studies, beside human alveolar epithelial cells, human and mouse dendritic cells mostly chosen for the study the IFNs response to HMPV infection [25, 26, 36] on human MDMs. In this study, we have investigated if type I and III IFNs affected gene induction and HMPV levels in human MDMs.

We found that pre-treatment with type I and III IFN can protect MDMs against viral infection more effective at 48 hours, especially if we prolonged the IFNs pre-stimulation duration up to 24 hours. It seems like prolonged treatment can stimulate sustained immune activation. In more detail, the kinetics of Viperin expression paralleled the kinetics of HMPV production along with IFNs in infected cells, suggesting that both IFN type I and III may be the potential provider to Viperin expression during HMPV infection.

Aside from that, we found the presence of CXCL-10 mRNAs in human MDMs, which is consistent with the result from Le Nouen et al. [77] who also confirmed the strong response of CXCL-10 by HMPV. Moreover, pre-treatment with IFN-λ1 can reduce the production of CXCL-10 which lessens the inflammatory response in HMPV-infected MDMs. Interestingly, in the first 24 hours of viral exposure, Viperin and CXCl-10 were highly induced by IFN-λ1 but not IFN-β, this is contradicted with prior research that type III IFN appeared to have lower in magnitude [30, 39, 41]. Further experiment regarding virus titer needs to be done in the future to confirm reduction of HMPV infectious in the infected cells after pre-treatment with IFNs.

Taken together, the study provides insight into the antiviral response induced by pre-treated IFNs is more efficiency at 48 hours exposure to the virus, which may imply strategies to find the suitable time for patient to receive treatment.

4.3 Role of Type I and III IFNs in Control of ISGs Gene Induction

To evaluate expression of ISGs by IFN-λ1 and IFN-β, we analyzed their kinetics in MDMs by using qRT-PCR. The data suggests that the majority of these ISG genes in this study were induced upon both type IFNs treatment. However, type I IFN signaling is illustrated by high potency of

ISGs expression with a more rapid kinetics, while type III IFN mediated antiviral protection expressed a moderate induction of ISGs and delayed 2 hours to reach the maximal compared to type I IFN. Our findings are consistent with prior research that found type III IFN to be less robust in producing ISGs than type I IFN [39, 41, 67, 78].

More detailed, IFN stimulation was sufficient to induce Viperin expression in MDMs, though IFN-λ1 was capable of inducing expression of Viperin, IFN-β were a potent activator. In contrary to Casazza et al. [41] who claimed that CXCL-10 was induced exclusively by IFN-β not IFN-λ (in mice intranasally), our result found the change in the production CXCL-10.

Via this experiment, we found that treatment with IFN-β can increase the levels of IL-6 mRNA while IFN-λ1 can lessen release of proinflammatory cytokines IL-6. This result can suggest a significant contribution of IFN type III to treat HMPV infection since prior research demonstrated that infections with RSV and HMPV expressed a correlation between high levels of IL-6 and disease severity in the host [79].

CH25H, a member of the ISG family, has been recently investigation and have been found to exhibit antiviral activities and affect in immunometabolism, though the mechanism behind it is still unclear. In this study, we characterized the expression of CH25H by type I and III IFNs in human MDMs. We found a noticeable elevation of CH25H gene expression in the cells in early viral exposure duration among the other interested ISGs when treatment with IFNs. This expression showed an early and transient induction of CH25H primarily upon stimulation by types I and III IFN, yet CH25H was more potently activated by type I IFN in comparison with type III counterpart. This result is different from prior research of Xiang et al. [80], who claimed that CH25H could not induced by IFNs type I on human MDMs and other cell lines such as Huh7 and A549 cells. However, our result is in line with the studies of Angakusuma et al. [54], showing that CH25H is quickly induced by type I IFN. Surprisingly, both Xiang et al. and Angakusuma et al. all used IFN-α on human MDMs but provided contradictory conclusion. This conflicting data could be explained in relation to concentration and timing in which Xiang et al. used IFN-α (100 IU/ml) at 8 h post-treatment while Angakusuma et al. used IFN-α (1000 IU/mL) at 4, 8, 24h. For further studies, both time and concentration must be unified.

4.4 The Impact of siIFNLR1 Transfection on IFN-treated or HMPV-Infected MDMs

To determine the role of type I and III IFN signaling in the regulation of ISGs expression, human MDMs were stimulated with IFN-λ1, or IFN-β. We found the siRNA targeting IFNLR1 mRNA used in this study was effectively silenced IFNLR1 mRNA expression. Elimination of type III receptor can abolish or at least reduce Viperin mRNA production in MDMs, so that IFNLR1 might mediate Viperin induction and hence be functional in MDMs. IFN- λ1 and IFN-β treatment resulted in a moderate induction of CXCL-10 transcription in the MDMs but apparently lesser than HMPV infection. The similar result was also observed for IL-6. This might suggest that other signaling pathway independent from type III IFN receptor-mediated signaling pathway is involved in the induction of IL-6 and CXCL-10 mRNA after stimulation with IFN-λ1. One possible causative might be type I IFN signaling, even though the levels were reduced by siRNA-transfection. IFNAR is still expressed so that when the cells sense siRNA as a viral by-product (via RIG/MDA5), it mounts an immune response producing IFN type I that could mediate ISGs induction. Consequently, presence of IFNAR could induce ISGs as we observed. This is especially true for CXCL-10, since type I IFN is exceptional in producing it [39, 41]. Taken together, since treating with type III IFN can induce less proinflammatory cytokine compare with type I IFNs, such that IFNLR1 is necessary in inducing Viperin, and controlling IL-6 and CXCL-10 expression. To sum up, this experiment still got a limitation during the analysis where we should compare with siAllStar with the same treatment to see the change of gene expression between un-transfection and transfection .

4.5 Ruxolitinib Down Regulates ISGs and Block the Pro-Inflammatory Cytokine IL-6

Ruxolitinib has significant potential in the treatment of various inflammatory diseases caused by JAK /STAT immune hyperactivation. However, JAK /STAT signaling is a primary pathway, so its blockage may lead to inhibition of various ISGs that benefit from antiviral activities, increasing the chance of opportunistic infections [81]. Our results have shown that ruxolitinib at 5 μM or 10

μM concentration is able to inhibit the production of the inflammatory cytokine IL -6 without impeding other cytokines such as viperine, CXCL-10 and CH25H on IFN-β treated MDMs. It should be noted that when treated with IFN-λ1 and IFN-β, only IFN-β is able to bypass the effect of ruxolitinib in inducing ISGs. This could be true for Viperin, as its gene expression can be regulated by IFN-independent pathways [46], or for CXCL-10, whose gene expression can be regulated by NF-κB-dependent pathways [82].

5 Conclusion

In summary, in this study we found that human MDMs express IFNLR1, and that IFN-λ1 induces in these cells, suggesting that the IFNLR1 in functional. Induction of ISG by type I and III IFNs different in magnitude and kinetics of ISG induction, although they induce a similar subset of genes. Among the ISGs of interest, we observed that CH25H was the first ISG to appear early after IFN stimulation in human MDMs. During stimulation, CH25H was more activated by type I IFN than type III. Future studies are needed to investigate the antiviral activity of CH25H. siRNA-mediated knockout of IFNLR1 was efficient and led to enhance HMPV replication. This suggests an important role for type III IFNs signaling in innate antimicrobial defense. In addition, we found that the JAK/STAT inhibitor reduced ISGs induction by type I and III IFNs. To sum up, the result in this thesis suggest that human MDMs express a functional IFNLR1.

6 References

1. Simoes, E.A.F., et al., *Acute Respiratory Infections in Children*, in *Disease Control Priorities in Developing Countries*, nd, et al., Editors. 2006: Washington (DC).
2. Panda, S., et al., *Human metapneumovirus: review of an important respiratory pathogen.* Int J Infect Dis, 2014. **25**: p. 45-52.
3. Williams, B.G., et al., *Estimates of world-wide distribution of child deaths from acute respiratory infections.* Lancet Infect Dis, 2002. **2**(1): p. 25-32.
4. van den Hoogen, B.G., et al., *A newly discovered human pneumovirus isolated from young children with respiratory tract disease.* Nat Med, 2001. **7**(6): p. 719-24.
5. Shafagati, N. and J. Williams, *Human metapneumovirus - what we know now.* F1000Research, 2018. **7**: p. 135-135.
6. Kahn, J.S., *Epidemiology of human metapneumovirus.* Clin Microbiol Rev, 2006. **19**(3): p. 546-57.
7. Williams, J.V., et al., *Human metapneumovirus and lower respiratory tract disease in otherwise healthy infants and children.* N Engl J Med, 2004. **350**(5): p. 443-50.

8. Weston, S. and M.B. Frieman, *Respiratory Viruses.* Encyclopedia of Microbiology, 2019: p. 85-101.
9. Hermos, C.R., S.O. Vargas, and A.J. McAdam, *Human metapneumovirus.* Clin Lab Med, 2010. **30**(1): p. 131-48.
10. Kutter, J.S., et al., *Transmission routes of respiratory viruses among humans.* Current Opinion in Virology, 2018. **28**: p. 142-151.
11. Haas, L.E., et al., *Human metapneumovirus in adults.* Viruses, 2013. **5**(1): p. 87-110.
12. Tollefson, S.J., R.G. Cox, and J.V. Williams, *Studies of culture conditions and environmental stability of human metapneumovirus.* Virus Res, 2010. **151**(1): p. 54-9.
13. Masante, C., et al., *The human metapneumovirus small hydrophobic protein has properties consistent with those of a viroporin and can modulate viral fusogenic activity.* J Virol, 2014. **88**(11): p. 6423-33.
14. Cespedes, P.F., et al., *Modulation of Host Immunity by the Human Metapneumovirus.* Clin Microbiol Rev, 2016. **29**(4): p. 795-818.
15. Bao, X., et al., *Human metapneumovirus small hydrophobic protein inhibits NF-kappaB transcriptional activity.* J Virol, 2008. **82**(16): p. 8224-9.
16. Le Nouen, C., et al., *Human metapneumovirus SH and G glycoproteins inhibit macropinocytosis-mediated entry into human dendritic cells and reduce CD4+ T cell activation.* J Virol, 2014. **88**(11): p. 6453-69.
17. Schildgen, V., et al., *Human Metapneumovirus: lessons learned over the first decade.* Clin Microbiol Rev, 2011. **24**(4): p. 734-54.
18. Kinder, J.T., et al., *Human metapneumovirus fusion protein triggering: Increasing complexities by analysis of new HMPV fusion proteins.* Virology, 2019. **531**: p. 248-254.
19. Feuillet, F., et al., *Ten years of human metapneumovirus research.* J Clin Virol, 2012. **53**(2): p. 97-105.
20. Aftab, S., et al., *Human Metapneumovirus (hMPV) Proteins, their Therapeutics and Vaccine Potentials.* Indian Journal of Health Sciences and Care, 2017. **4**: p. 126.
21. Kitagawa, Y., et al., *Human metapneumovirus M2-2 protein inhibits viral transcription and replication.* Microbes Infect, 2010. **12**(2): p. 135-45.
22. De Andrea, M., et al., *The interferon system: an overview.* Eur J Paediatr Neurol, 2002. **6 Suppl A**: p. A41-6; discussion A55-8.
23. Razaghi, A., L. Owens, and K. Heimann, *Review of the recombinant human interferon gamma as an immunotherapeutic: Impacts of production platforms and glycosylation.* J Biotechnol, 2016. **240**: p. 48-60.
24. Sen, G.C., *Viruses and interferons.* Annu Rev Microbiol, 2001. **55**: p. 255-81.
25. Essaidi-Laziosi, M., et al., *Interferon-Dependent and Respiratory Virus-Specific Interference in Dual Infections of Airway Epithelia.* Sci Rep, 2020. **10**(1): p. 10246.
26. Egli, A., et al., *The impact of the interferon-lambda family on the innate and adaptive immune response to viral infections.* Emerg Microbes Infect, 2014. **3**(7): p. e51.
27. Schneider, W.M., M.D. Chevillotte, and C.M. Rice, *Interferon-stimulated genes: a complex web of host defenses.* Annu Rev Immunol, 2014. **32**: p. 513-45.
28. Hastings, A.K., et al., *Role of type I interferon signaling in human metapneumovirus pathogenesis and control of viral replication.* J Virol, 2015. **89**(8): p. 4405-20.

29. Razaghi, A., L. Owens, and K. Heimann, *Review of the recombinant human interferon gamma as an immunotherapeutic: Impacts of production platforms and glycosylation.* Journal of Biotechnology, 2016. **240**: p. 48-60.
30. Lazear, H.M., J.W. Schoggins, and M.S. Diamond, *Shared and Distinct Functions of Type I and Type III Interferons.* Immunity, 2019. **50**(4): p. 907-923.
31. Sheppard, P., et al., *IL-28, IL-29 and their class II cytokine receptor IL-28R.* Nat Immunol, 2003. **4**(1): p. 63-8.
32. Syedbasha, M. and A. Egli, *Interferon Lambda: Modulating Immunity in Infectious Diseases.* Front Immunol, 2017. **8**: p. 119.
33. Witte, K., et al., *Despite IFN-lambda receptor expression, blood immune cells, but not keratinocytes or melanocytes, have an impaired response to type III interferons: implications for therapeutic applications of these cytokines.* Genes Immun, 2009. **10**(8): p. 702-14.
34. Lasfar, A., & Cohen-Solal, K. A. *Emergence of IFN-lambda as a Potential Antitumor Agent*. Targets in gene therapy 2011 [cited 2021 06]; Available from: https://www.intechopen.com/books/targets-in-gene-therapy/emergence-of-ifn-lambda-as-a-potential-antitumor-agent.
35. O'Connor, K.S., et al., *IFNL3/4 genotype is associated with altered immune cell populations in peripheral blood in chronic hepatitis C infection.* Genes Immun, 2016. **17**(6): p. 328-34.
36. Uche, I.K. and A. Guerrero-Plata, *Interferon-Mediated Response to Human Metapneumovirus Infection.* Viruses, 2018. **10**(9).
37. Takeuchi, O. and S. Akira, *Pattern recognition receptors and inflammation.* Cell, 2010. **140**(6): p. 805-20.
38. Hoebe, K. and B. Beutler, *TRAF3: a new component of the TLR-signaling apparatus.* Trends Mol Med, 2006. **12**(5): p. 187-9.
39. Stanifer, M.L., K. Pervolaraki, and S. Boulant, *Differential Regulation of Type I and Type III Interferon Signaling.* International Journal of Molecular Sciences, 2019. **20**(6).
40. Jewell, N.A., et al., *Lambda interferon is the predominant interferon induced by influenza A virus infection in vivo.* J Virol, 2010. **84**(21): p. 11515-22.
41. Casazza, R.L. and H.M. Lazear, *Why Is IFN-λ Less Inflammatory? One IRF Decides.* Immunity, 2019. **51**(3): p. 415-417.
42. Janeway CA Jr, T.P., Walport M, et al., *The major histocompatibility complex and its functions*. 5th ed. Immunobiology: The Immune System in Health and Disease. 2001, New York: Garland Science.
43. Ferrington, D.A. and D.S. Gregerson, *Immunoproteasomes: structure, function, and antigen presentation.* Prog Mol Biol Transl Sci, 2012. **109**: p. 75-112.
44. Schoggins, J.W., *Interferon-Stimulated Genes: What Do They All Do?* Annu Rev Virol, 2019. **6**(1): p. 567-584.
45. Liu, S.Y., et al., *Interferon-inducible cholesterol-25-hydroxylase broadly inhibits viral entry by production of 25-hydroxycholesterol.* Immunity, 2013. **38**(1): p. 92-105.
46. Duschene, K.S. and J.B. Broderick, *Viperin: a radical response to viral infection.* Biomol Concepts, 2012. **3**(3): p. 255-266.
47. Fitzgerald, K.A., *The interferon inducible gene: Viperin.* J Interferon Cytokine Res, 2011. **31**(1): p. 131-5.

48. Seo, J.Y., R. Yaneva, and P. Cresswell, *Viperin: a multifunctional, interferon-inducible protein that regulates virus replication.* Cell Host Microbe, 2011. **10**(6): p. 534-9.
49. Ng, L.F.P. and J.A. Hiscox, *Viperin Poisons Viral Replication.* Cell Host Microbe, 2018. **24**(2): p. 181-183.
50. Wang, X., E.R. Hinson, and P. Cresswell, *The interferon-inducible protein viperin inhibits influenza virus release by perturbing lipid rafts.* Cell Host Microbe, 2007. **2**(2): p. 96-105.
51. Jumat, M.R., et al., *Viperin protein expression inhibits the late stage of respiratory syncytial virus morphogenesis.* Antiviral Res, 2015. **114**: p. 11-20.
52. Cyster, J.G., et al., *25-Hydroxycholesterols in innate and adaptive immunity.* Nat Rev Immunol, 2014. **14**(11): p. 731-43.
53. Zhao, J., et al., *Multifaceted Functions of CH25H and 25HC to Modulate the Lipid Metabolism, Immune Responses, and Broadly Antiviral Activities.* Viruses, 2020. **12**(7).
54. Anggakusuma, et al., *Interferon-inducible cholesterol-25-hydroxylase restricts hepatitis C virus replication through blockage of membranous web formation.* Hepatology, 2015. **62**(3): p. 702-14.
55. Park, K. and A.L. Scott, *Cholesterol 25-hydroxylase production by dendritic cells and macrophages is regulated by type I interferons.* J Leukoc Biol, 2010. **88**(6): p. 1081-7.
56. Olsen, B.N., et al., *25-Hydroxycholesterol increases the availability of cholesterol in phospholipid membranes.* Biophys J, 2011. **100**(4): p. 948-56.
57. Lange, Y., J. Ye, and F. Strebel, *Movement of 25-hydroxycholesterol from the plasma membrane to the rough endoplasmic reticulum in cultured hepatoma cells.* J Lipid Res, 1995. **36**(5): p. 1092-7.
58. Fessler, M.B., *The Intracellular Cholesterol Landscape: Dynamic Integrator of the Immune Response.* Trends Immunol, 2016. **37**(12): p. 819-830.
59. Gálvez, N.M.S., et al., *Host Components That Modulate the Disease Caused by hMPV.* Viruses, 2021. **13**(3): p. 519.
60. Dinwiddie, D.L. and K.S. Harrod, *Human metapneumovirus inhibits IFN-alpha signaling through inhibition of STAT1 phosphorylation.* Am J Respir Cell Mol Biol, 2008. **38**(6): p. 661-70.
61. Han, H., *RNA Interference to Knock Down Gene Expression.* Methods Mol Biol, 2018. **1706**: p. 293-302.
62. Dheda, K., et al., *Validation of housekeeping genes for normalizing RNA expression in real-time PCR.* Biotechniques, 2004. **37**(1): p. 112-4, 116, 118-9.
63. *Guide to Performing Relative Quantitation of Gene Expression Using Real-Time Quantitative PCR (Applied Biosystems)*. 2008; Available from: https://assets.thermofisher.com/TFS-Assets/LSG/manuals/cms_042380.pdf.
64. Santer, D.M., et al., *Differential expression of interferon-lambda receptor 1 splice variants determines the magnitude of the antiviral response induced by interferon-lambda 3 in human immune cells.* PLoS Pathog, 2020. **16**(4): p. e1008515.
65. Santer, D.M., et al., *A novel method for detection of IFN-lambda 3 binding to cells for quantifying IFN-lambda receptor expression.* J Immunol Methods, 2017. **445**: p. 15-22.
66. Voigt, E.A. and J. Yin, *Kinetic Differences and Synergistic Antiviral Effects Between Type I and Type III Interferon Signaling Indicate Pathway Independence.* Journal of interferon & cytokine research : the official journal of the International Society for Interferon and Cytokine Research, 2015. **35**(9): p. 734-747.

67. Pervolaraki, K., et al., *Differential induction of interferon stimulated genes between type I and type III interferons is independent of interferon receptor abundance.* PLoS Pathog, 2018. **14**(11): p. e1007420.
68. Forero, A., et al., *Differential Activation of the Transcription Factor IRF1 Underlies the Distinct Immune Responses Elicited by Type I and Type III Interferons.* Immunity, 2019. **51**(3): p. 451-464 e6.
69. Zarogoulidis, P., et al., *Interleukin-6 cytokine: a multifunctional glycoprotein for cancer.* Immunome Res, 2013. **9**(62): p. 16535.
70. Choy, E. and S. Rose-John, *Interleukin-6 as a Multifunctional Regulator: Inflammation, Immune Response, and Fibrosis.* Journal of Scleroderma and Related Disorders, 2017. **2**(2_suppl): p. S1-S5.
71. Dienz, O. and M. Rincon, *The effects of IL-6 on CD4 T cell responses.* Clin Immunol, 2009. **130**(1): p. 27-33.
72. Liu, S.Y., et al., *Systematic identification of type I and type II interferon-induced antiviral factors.* Proc Natl Acad Sci U S A, 2012. **109**(11): p. 4239-44.
73. Read, S.A., et al., *Zinc is a potent and specific inhibitor of IFN-λ3 signalling.* Nature Communications, 2017. **8**(1): p. 15245.
74. Read, S.A., et al., *Macrophage Coordination of the Interferon Lambda Immune Response.* Front Immunol, 2019. **10**: p. 2674.
75. Mubarak, R.A., et al., *Comparison of pro- and anti-inflammatory responses in paired human primary airway epithelial cells and alveolar macrophages.* Respir Res, 2018. **19**(1): p. 126.
76. Liu, B.S., H.L. Janssen, and A. Boonstra, *IL-29 and IFNalpha differ in their ability to modulate IL-12 production by TLR-activated human macrophages and exhibit differential regulation of the IFNgamma receptor expression.* Blood, 2011. **117**(8): p. 2385-95.
77. Le Nouen, C., et al., *Infection and maturation of monocyte-derived human dendritic cells by human respiratory syncytial virus, human metapneumovirus, and human parainfluenza virus type 3.* Virology, 2009. **385**(1): p. 169-82.
78. Levy, D.E., I.J. Marie, and J.E. Durbin, *Induction and function of type I and III interferon in response to viral infection.* Curr Opin Virol, 2011. **1**(6): p. 476-86.
79. Mitzel, D.N., et al., *Human metapneumovirus inhibits the IL-6-induced JAK/STAT3 signalling cascade in airway epithelium.* The Journal of general virology, 2014. **95**(Pt 1): p. 26-37.
80. Xiang, Y., et al., *Identification of Cholesterol 25-Hydroxylase as a Novel Host Restriction Factor and a Part of the Primary Innate Immune Responses against Hepatitis C Virus Infection.* J Virol, 2015. **89**(13): p. 6805-16.
81. Goker Bagca, B. and C. Biray Avci, *The potential of JAK/STAT pathway inhibition by ruxolitinib in the treatment of COVID-19.* Cytokine Growth Factor Rev, 2020. **54**: p. 51-62.
82. Vazirinejad, R., et al., *The biological functions, structure and sources of CXCL10 and its outstanding part in the pathophysiology of multiple sclerosis.* Neuroimmunomodulation, 2014. **21**(6): p. 322-30.

7 Supplement

A)

Sample	sIFNLR1 Ct Mean	mIFNLR1 Ct Mean	Concentration	Log conc.
undiluted	29.89	26.61	0.00	0.00
1:10	33.27	30.58	0.10	-1.00
1:100	36.11	33.53	0.01	-2.00

	sIFNLR1	mIFNLR1
Slope	-3.1	-3.5
R Squared	1.00	0.99
Efficiency (%)	109.6	94.7

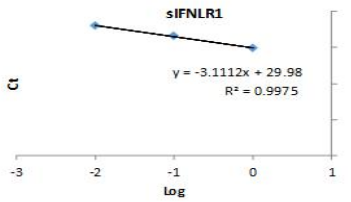

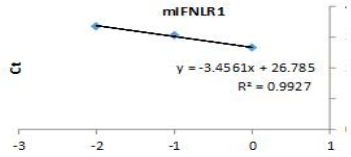

B)

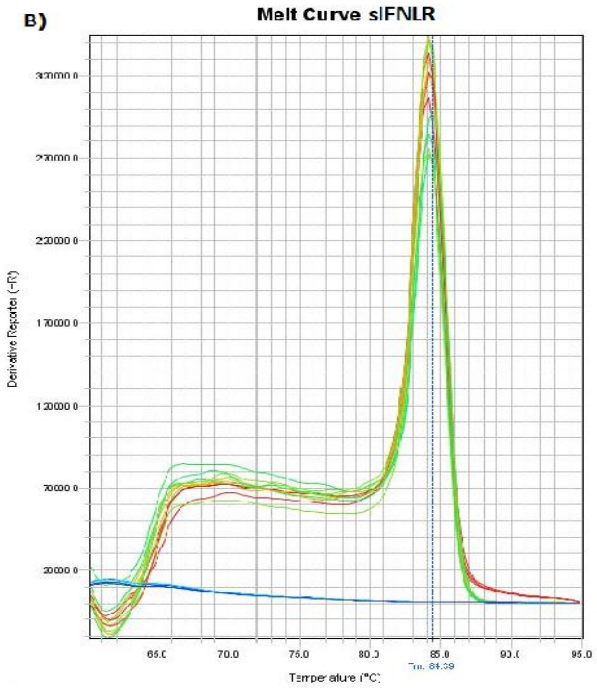

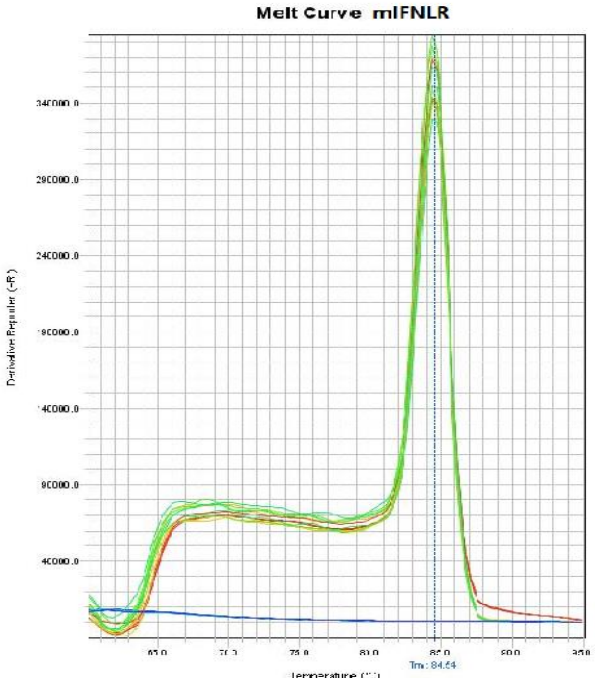

Supplementary Figure 1 Primer validation for sIFNLR1 and mIFNLR1. A) The primer efficiency for the PCR quantification of the IFNLR gene was determined on MDMs using a 10-fold dilution series. The respective correlation coefficients (R^2) are indicated. B) The PCR products from A) were used to generate a melting curve analysis. All PCR products melt around 84 °C which indicates the breakdown of only one PCR product, no detect of off-target amplification or contamination.

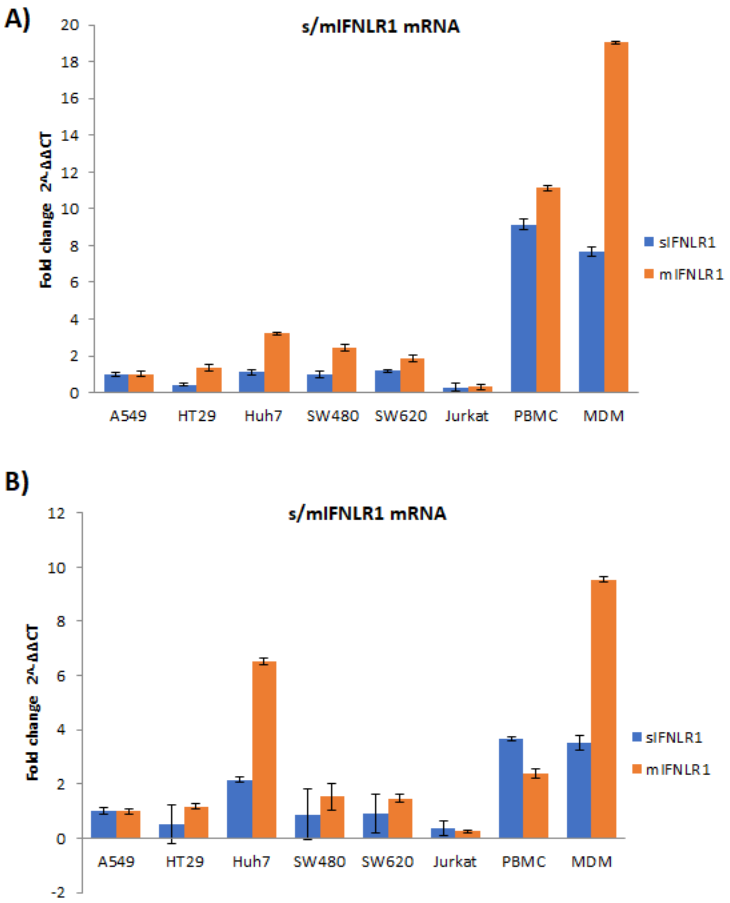

Supplementary Figure 2 Expression of IFNLR1 variant (sIFNLR1 and mIFNLR1) on different cell types. RT-qPCR was used to determine the relative expression of mIFNLR1 and sIFNLR1 forms of IFNLR1 with normalization to the reference gene A) GAPDH/TBP and B) TBP/β-actin. The data showed for A549, Jurkat, PBMC, HT29, Huh7, SW480, SW620, and MDM. Relative expression values were calculated normalized to A549 (control). Data shows $2^{-\Delta\Delta Ct} \pm SD$ *(n = 3).*

A)

Sample	Ct Mean	Concentration	Log conc.
undiluted	18.90	0.00	0.00
1:10	21.50	0.10	-1.00
1:50	24.46	0.02	-1.70
1:100	25.52	0.01	-2.00

	CXCL-10
Slope	-3.3
R Squared	0.99
Efficiency (%)	**99.1**

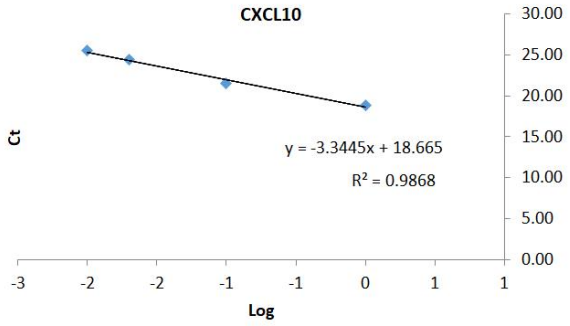

B)

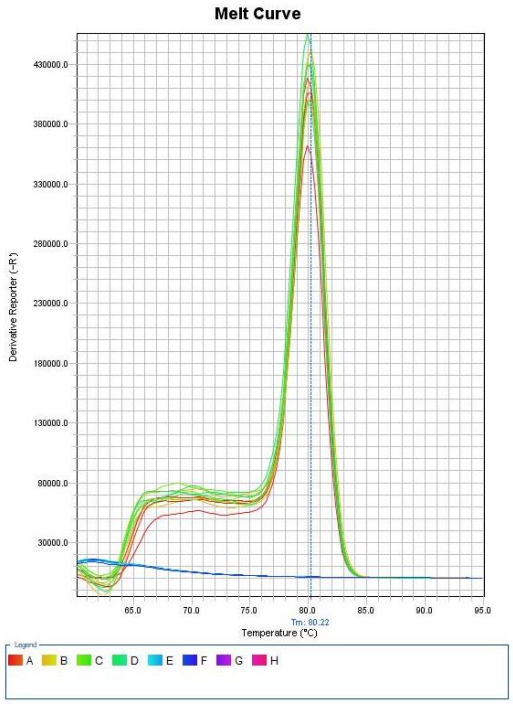

Supplementary Figure 3 Primer validation for CXCL-10. A) The primer efficiency for the PCR quantification of the IFNLR gene was determined on MDMs using a dilution series. The respective correlation coefficients (R^2) are indicated. B) The PCR products from A) were used to generate a melting curve analysis. All PCR products melt around 80 °C which indicates the breakdown of only one PCR product, no detect of off-target amplification or contamination.

A)

Sample	CH25H Ct Mean	Concentration	Log conc.
undiluted	24.60	0.00	0.00
1:10	27.86	0.10	-1.00
1:50	30.14	0.02	-1.70
1:100	31.08	0.01	-2.00

	CH25H
Slope	-3.2
R Squared	1.00
Efficiency (%)	103.3

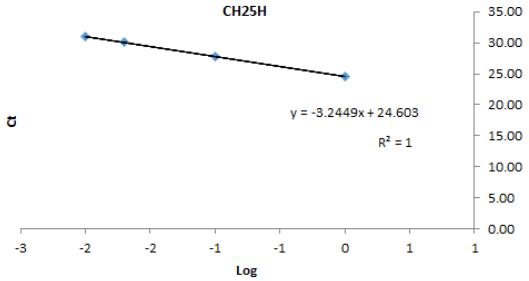

B)

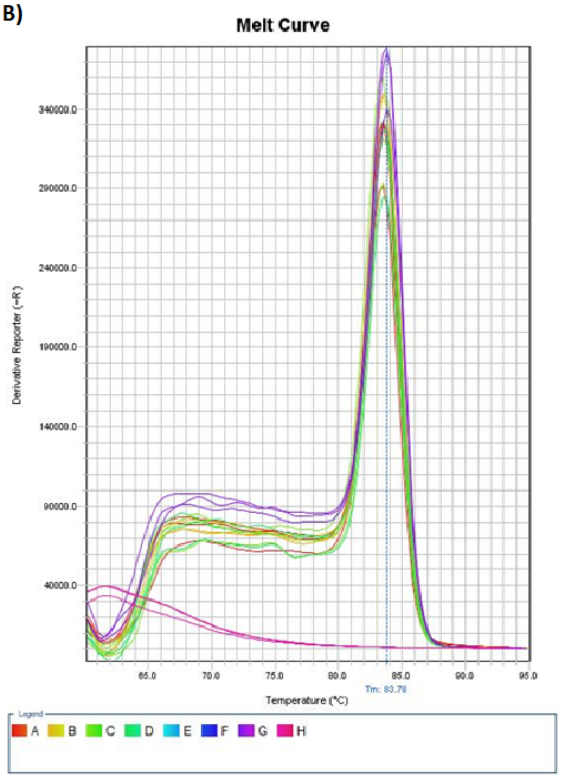

Supplementary Figure 4 Primer validation for CH25H. A) The primer efficiency for the PCR quantification of the IFNLR gene was determined on MDMs using a 10-fold dilution series. The respective correlation coefficients (R^2) are indicated. B) The PCR products from A) were used to generate a melting curve analysis. All PCR products melt around 83 °C which indicates the breakdown of only one PCR product, no detect of off-target amplification or contamination.

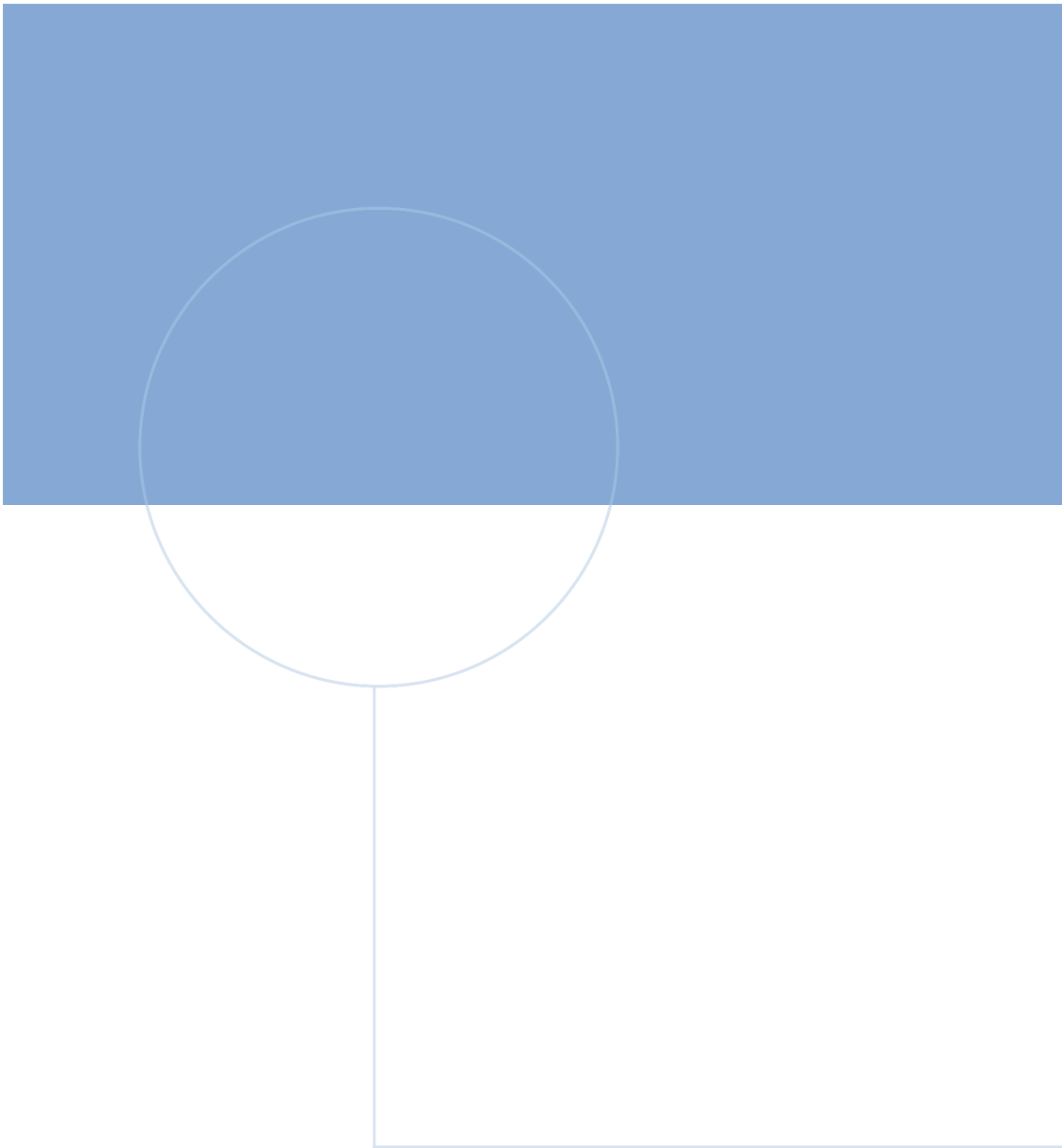

NTNU

Norwegian University of
Science and Technology